

AMEND: A Model Explaining Neutrino masses and Dark matter testable at the LHC and MEG

Yasaman Farzan

*School of Physics, Institute for research in fundamental sciences (IPM), P.O. Box
19395-5531, Tehran, Iran
Email: yasaman@theory.ipm.ac.ir*

Silvia Pascoli

*Institute for Particle Physics Phenomenology (IPPP), Department of Physics, Durham
University, Durham DH1 3LE, UK
Email: silvia.pascoli@durham.ac.uk*

Michael A. Schmidt

*Institute for Particle Physics Phenomenology (IPPP), Department of Physics, Durham
University, Durham DH1 3LE, UK
Email: m.a.schmidt@durham.ac.uk*

ABSTRACT: Despite being very successful in explaining the wide range of precision experimental results obtained so far, the Standard Model (SM) of elementary particles fails to address two of the greatest observations of the recent decades: tiny but nonzero neutrino masses and the well-known problem of missing mass in the Universe. Typically the new models beyond the SM explain only one of these observations. Instead, in the present article, we take the view that they both point towards the same new extension of the Standard Model. The new particles introduced are responsible simultaneously for neutrino masses and for the dark matter of the Universe. The stability of dark matter and the smallness of neutrino masses are guaranteed by a $U(1)$ global symmetry, broken to a remnant \mathbb{Z}_2 . The canonical seesaw mechanism is forbidden and neutrino masses emerge at the loop level being further suppressed by the small explicit breaking of the $U(1)$ symmetry. The new particles and interactions are invoked at the electroweak scale and lead to rich phenomenology in colliders, in lepton flavour violating rare decays and in direct and indirect dark matter searches, making the model testable in the coming future.

KEYWORDS: [Beyond Standard Model](#), [Neutrino Physics](#), [Cosmology of Theories beyond the SM](#).

Contents

1. Introduction	1
2. The Model	3
3. Neutral Scalar Masses	5
4. Lepton Sector	7
4.1 Neutrino Masses	7
4.2 Lepton Flavour Violating Rare Decays	10
4.3 Anomalous Magnetic Moment of the Muon	11
5. Dark Matter	11
5.1 Dark Matter Abundance in the Universe	12
5.2 Direct Dark Matter Searches	17
5.3 Indirect Dark Matter Searches	21
6. Other Constraints on the Model and Laboratory Signatures	22
6.1 Electroweak Precision Tests	22
6.2 Signatures at Colliders	23
7. Conclusions	24
A. Scalar Mass Spectrum	26

1. Introduction

Despite all its triumphs, the Standard Model (SM) of elementary particles fails to explain two of the greatest observations of the recent decades: tiny but nonzero neutrino masses and the missing mass of the Universe commonly explained by Dark Matter (DM). Various models beyond the Standard Model (BSM) have been developed to explain each of these mysteries separately. On the contrary these two phenomena may be linked and explained within a single scenario [1, 2, 3]. In the present article we will explore this possibility and propose an extension of the Standard Model in which the new particles and interactions are simultaneously responsible for the dark matter of the Universe and neutrino masses. We call our model AMEND which stands for “A Model Explaining Neutrino masses and Dark matter”. We introduce a $U(1)_X$ global symmetry which is broken to a remnant \mathbb{Z}_2 . The latter symmetry distinguishes the new particles from the SM ones and is responsible for the stability of dark matter. At the same time, it forbids the canonical seesaw mechanism

and left-handed neutrinos do not acquire a Dirac mass. Neutrino masses arise at the loop level and are suppressed by small terms which explicitly break the $U(1)_X$ symmetry.

More concretely, we introduce two additional electroweak doublets R and R' with opposite hypercharges. These Weyl fermions together can be regarded as a Dirac four component spinor. Moreover, we add an electroweak scalar triplet Δ and a complex singlet ϕ which do not acquire vacuum expectation values (VEVs). The lightest neutral scalar, which is mainly the singlet ϕ with a small admixture of the neutral component of Δ , will play the role of the DM particle. We expect the mass value for DM to be around the electroweak scale so the DM in our model can be categorised as a weakly interacting massive particle (WIMP). Smaller values can be obtained if fine-tuning is allowed in the DM mass term. The Yukawa coupling involving Δ is the lepton number violating interaction which leads to Majorana neutrino masses. The neutrino masses are generated at one loop and are proportional to the mass of the new fermionic doublet which needs to be at the electroweak scale or higher. The model presented in this paper belongs to the class of models for which the neutrino mass is generated radiatively (see *e.g.* [4]). The low neutrino mass scale therefore requires a further suppression, in addition to the loop-factor, by either suppressing the Yukawa coupling or by requiring a cancellation between the various contributions. In our model both of these requirements are simultaneously enforced by a continuous Abelian symmetry $U(1)_X$ which forbids the neutrino masses. Its explicit breaking to a residual \mathbb{Z}_2 symmetry leads to small neutrino masses and a stable DM particle at the same time.

In our model, DM is produced thermally in the Early Universe. We explore the various allowed annihilation channels which can proceed via R - R' , Z or Higgs exchange, in order to reproduce the observed amount of dark matter $\Omega_{\text{DM}} h^2 = 0.1131 \pm 0.0034$ [5]. We find that in the parameter range of interest, the dark matter annihilation through s -channel Higgs exchange dominates over the other channels. Dark matter is being searched for both directly, looking for the recoil of nucleons/electrons due to DM scattering in detectors, and indirectly, observing the products of DM annihilations (photons, positrons, neutrinos, anti-protons, anti-deuteron) in overdense regions in the galaxy or inside astrophysical objects such as the Sun or the Earth. No positive signal has been found in direct searches except for the two events in CDMS-II [6] and the DAMA experiment which has reported a positive signal at 8.2σ [7]. Very recently, the CoGeNT collaboration [8] has found an indication for excess of events that might be due to scattering of light DM off the nuclei. The first analysis of the XENON100 experiment [9] excludes all positive DM signals, however the interpretation of the data depends on the astrophysical uncertainties [10] as well as the effective light yield in the low mass region [11]. We will consider these possible signals for DM detection and check whether they can be accommodated in our model. In the case of DAMA, we look into two possible explanations, by either light dark matter or by the inelastic scattering scenario. As our candidate is a quasi-singlet coupled to the Higgs boson, the interactions which induce the dark matter annihilations at freeze-out are also responsible for elastic or inelastic scattering off nuclei, relevant for direct dark matter searches. In some cases the cross sections of the two processes, annihilations and scattering off nuclei, are related.

All new particles are typically expected to have masses around the electroweak scale

particle	$SU(3)_c$	$SU(2)_L$	$U(1)_Y$	
Q_L	3	2	1/6	fermion
u_R	3	1	2/3	
d_R	3	1	-1/3	
ℓ_L	1	2	-1/2	
e_R	1	1	-1	
$R = R_R$	1	2	-1/2	
$R' = R'_R$	1	2	1/2	
H	1	2	1/2	scalar
Δ	1	3	1	
ϕ	1	1	0	

Table 1: Particle content and gauge quantum numbers.

and to couple to the SM particles at tree level leading to rich phenomenology which makes the model testable in the near future. We therefore investigate several experimental bounds including the invisible decay width of the Z into DM pair (if kinematically allowed), the branching ratios of Lepton Flavour Violating (LFV) rare decays and the anomalous magnetic moment of the muon. Furthermore, we comment on the possible signatures at the LHC. It is possible to correlate the flavour structure of the couplings measured at the LHC with the neutrino mass matrix and the data from LFV rare decay searches.

The paper is organised as follows. In sec. 2, the model is presented. In sec. 3, the neutral scalar sector is analysed. In sec. 4, the neutrino mass generation at one loop level as well as effects on the LFV rare decays and magnetic dipole moment of the muon are discussed. In sec. 5, different processes that can give rise to annihilation of dark matter are explored. A discussion of the possibilities of direct and indirect dark matter detection is also included. In sec. 6, experimental constraints from electroweak precision tests as well as possible collider signatures are studied. Finally, in sec. 7, results are summarised.

2. The Model

In order to explain neutrino masses and dark matter, we extend the SM with two additional scalar fields, and one vector-like fermionic doublet. The complete particle content of the model and the SM quantum numbers are summarised in Tab. 1. More specifically, the scalar sector of the model contains three fields:

- the SM Higgs doublet which is indicated by H in the following;
- a complex field, $\phi \equiv (\phi_1 + i\phi_2)/\sqrt{2}$, which is a singlet of $SU(2)_L \times U(1)_Y$;
- and a triplet scalar field Δ :

$$\Delta = \begin{bmatrix} \frac{\Delta^+}{\sqrt{2}} & \Delta^{++} \\ \Delta^0 & -\frac{\Delta^+}{\sqrt{2}} \end{bmatrix}, \quad (2.1)$$

where the neutral component can be decomposed as $\Delta^0 = (\Delta_1 + i\Delta_2)/\sqrt{2}$, with Δ_i being real fields.

In the fermionic sector, the added vector-like $SU(2)_L$ doublet is described by two Weyl fermion $SU(2)_L$ doublets, $R^T = (\nu_R \ E_R^-)$ and $(R')^T = (E_R^+ \ \nu'_R)$.

With this particle content, a model enjoying a very high level of symmetry can be constructed. We consider a Lagrangian which preserves the SM gauge group as well as $U(1)_\ell$ of lepton number, $U(1)_\phi$ under which only ϕ is charged, a similar $U(1)_\Delta$ for Δ and $U(1)_R$ under which R and R' have opposite quantum numbers. Let us define

$$G \equiv U(1)_R \times U(1)_\phi \times U(1)_\Delta \times U(1)_\ell . \quad (2.2)$$

The G -preserving part of the scalar potential is given by

$$\begin{aligned} \mathcal{V} = & -\mu_H^2 H^\dagger H + \mu_\Delta^2 \text{tr}(\Delta^\dagger \Delta) + \mu_\phi^2 \phi^\dagger \phi \\ & + \frac{\lambda}{4} (H^\dagger H)^2 + \frac{\lambda_\phi}{4} (\phi^\dagger \phi)^2 + \frac{\lambda_{\Delta 1}}{2} \left(\text{tr} \Delta^\dagger \Delta \right)^2 + \frac{\lambda_{\Delta 2}}{2} \text{tr}(\Delta^\dagger [\Delta^\dagger, \Delta] \Delta) \\ & + \lambda_{H\Delta 1} H^\dagger H \text{tr}(\Delta^\dagger \Delta) + \lambda_{H\Delta 2} H^\dagger [\Delta^\dagger, \Delta] H + \lambda_{\phi\Delta} \phi^\dagger \phi \text{tr}(\Delta^\dagger \Delta) + \lambda_{H\phi} \phi^\dagger \phi H^\dagger H , \end{aligned} \quad (2.3)$$

and the fermionic part contains the Dirac mass term of the vector-like doublet

$$-\mathcal{L}_R = m_{RR} (R'^C)^\dagger \cdot R + \text{h.c.} , \quad (2.4)$$

where $(R'^C)^T = (\nu'_R{}^C \ - (E_R^+)^C)$. In order to avoid present collider bounds, we require m_{RR} to be larger than ~ 100 GeV. For definiteness we will take $m_{RR} = 300$ GeV, unless otherwise stated. Terms in Eqs. (2.3) and (2.4) constitute the most general renormalisable gauge invariant Lagrangian preserving G that can be added to the SM Lagrangian.

Among all possible $U(1)$ subgroups of G which can be obtained by assigning different possible charges to the fields, we list a number of symmetries that are of particular interest in Tab. 2. Notice that the quarks and the SM Higgs field have zero quantum numbers under these symmetries. We assume a hierarchical pattern for the breaking of the group. First at a very high energy, Λ_h , the group G breaks to $U(1)_X$ under which the fields are charged as in Tab. 2. Note that $G_{\text{SM}} \times U(1)_X$ is anomaly-free as the new fermionic doublet is vector-like. The terms which arise after $G \rightarrow U(1)_X$ are

$$\mathcal{V}_{H\Delta\phi} = \lambda_{H\Delta\phi} H^T i\sigma_2 \Delta^\dagger H \phi^\dagger + \text{h.c.} \quad (2.5a)$$

$$-\mathcal{L}_{\ell_L\phi} = g_\alpha \phi^\dagger R^\dagger \ell_{L\alpha} + \text{h.c.} . \quad (2.5b)$$

After electroweak symmetry breaking, the first term will induce mixing between ϕ and Δ . The second term introduces a coupling between the new sector and the leptonic doublet.

This $U(1)_X$ symmetry is eventually broken into a residual \mathbb{Z}_2 , under which SM particles are even and the new states are odd. The \mathbb{Z}_2 , being exact, forbids a Dirac mass term of form $R^\dagger \ell_{L\alpha}$ for neutrinos and neutrino masses cannot therefore arise from the seesaw mechanism.

Moreover, it guarantees the stability of the lightest new particle which is a potential dark matter candidate. At low energy, we expect a theory which is nearly $U(1)_X$ -conserving with small breaking terms which preserve \mathbb{Z}_2 . We assume this breaking to be explicit for the purpose of the present study. Notice that the terms $\mathcal{L}_{\ell_L\phi}$ and $\mathcal{V}_{H\Delta\phi}$ respect $U(1)_X$ and are not therefore suppressed. The $U(1)_X$ -violating contributions to the scalar potential are

$$\widetilde{\mathcal{V}}_{\text{scalar}} = \tilde{\lambda}_{H\Delta\phi} H^T i\sigma_2 \Delta^\dagger H\phi + \tilde{\mu}_\phi^2 \phi^2 + \tilde{\lambda}_{\phi 1} \phi^4 + \tilde{\lambda}_{\phi 2} \phi^3 \phi^\dagger + \tilde{\lambda}_{H\phi} H^\dagger H \phi^2 + \tilde{\lambda}_{\Delta\phi} \text{tr} \Delta^\dagger \Delta \phi^2 + \text{h.c.} . \quad (2.6)$$

The new Weyl fermions R and R' couple to the SM leptons with two additional \mathbb{Z}_2 -preserving terms

$$-\widetilde{\mathcal{L}}_{\ell_L\phi} = \tilde{g}_\alpha \phi R^\dagger \ell_{L\alpha} + \text{h.c.} \quad \text{and} \quad -\widetilde{\mathcal{L}}_{\ell_L\Delta} = (\tilde{g}_\Delta)_\alpha R'^\dagger \cdot \Delta \cdot \ell_{L\alpha} + \text{h.c.} . \quad (2.7)$$

Due to the assumed breaking pattern of the G symmetry, we have the hierarchy $g \gg \tilde{g}, \tilde{g}_\Delta$ and $\lambda_{H\Delta\phi} \gg \tilde{\lambda}_{H\Delta\phi}$. The freedom of a global phase transformation of ϕ and Δ can be used to set the phases of $\lambda_{H\Delta\phi}$ and $\tilde{\mu}_\phi^2$ to zero. Moreover, the phases of g_α can in general be absorbed by $\ell_{L\alpha}$. Thus, the $U(1)_X$ -preserving part as well as the mass terms can be made real. In this basis, \tilde{g}_α and $(\tilde{g}_\Delta)_\alpha$ can in general be complex leading to CP-violating Majorana and Dirac phases in the neutrino mass matrix. In this paper, for simplicity we restrict our analysis to the CP conserving case. Notice that, in general, the couplings $\tilde{\lambda}_{\phi 1}$, $\tilde{\lambda}_{\phi 2}$, $\tilde{\lambda}_{H\phi}$, $\tilde{\lambda}_{\Delta\phi}$, $\tilde{\lambda}_{H\Delta\phi}$ can be either positive or negative. The couplings have to be taken in a range such that the potential is stable at infinity. Since the $\tilde{\lambda}_{\phi 1}$, $\tilde{\lambda}_{\phi 2}$, $\tilde{\lambda}_{H\phi}$, $\tilde{\lambda}_{\Delta\phi}$ and $\tilde{\lambda}_{H\Delta\phi}$ couplings are much smaller than the corresponding $U(1)_X$ -conserving terms, the potential remains stable regardless of their sign. Unless otherwise specified, we take these couplings to be positive in our studies. A similar analysis and similar results could be obtained for negative couplings.

3. Neutral Scalar Masses

The parameters of the model can be chosen such that only the SM Higgs field develops a vacuum expectation value, that is

$$\langle \phi_1 \rangle = \langle \phi_2 \rangle = \langle \Delta_1 \rangle = \langle \Delta_2 \rangle = 0 . \quad (3.1)$$

particle	$U(1)_X$	\mathbb{Z}_2	$U(1)_{L1}$	$U(1)_{L2}$	$U(1)_{L3}$
ℓ_L	0	+	+1	-1	+1
e_R	0	+	-1	+1	-1
R	+1	-	+1	+1	+1
R'	-1	-	-1	-1	-1
Δ	+1	-	0	0	-2
ϕ	-1	-	0	0	0
breaking terms	$\widetilde{\mathcal{V}}_{\text{scalar}}, \widetilde{\mathcal{L}}_{\ell_L\phi}, \widetilde{\mathcal{L}}_{\ell_L\Delta}$	none	$\widetilde{\mathcal{L}}_{\ell_L\Delta}$	$\mathcal{L}_{\ell_L\phi}, \widetilde{\mathcal{L}}_{\ell_L\phi}$	$\lambda_{H\Delta\phi}, \tilde{\lambda}_{H\Delta\phi}$

Table 2: Specific $U(1)$ sub-groups of G and associated particle quantum numbers. Indicated are also the terms in the full Lagrangian which violate each symmetry.

As a result, the \mathbb{Z}_2 symmetry is preserved. The \mathbb{Z}_2 symmetry prevents mixing between the new scalars and the SM Higgs but the $\lambda_{H\Delta\phi}$ and $\tilde{\lambda}_{H\Delta\phi}$ couplings in $\mathcal{V}_{H\Delta\phi}$ and $\tilde{\mathcal{V}}_{H\Delta\phi}$ lead to mixing between ϕ and the neutral component of Δ . There are four massive neutral scalar fields in the model, $\delta_{1,2,3,4}$, with masses respectively given by

$$M_1^2 \simeq m_\phi^2 - \frac{m_{\phi\Delta}^4}{m_\Delta^2 - m_\phi^2} - \tilde{m}_\phi^2 - 2\frac{m_{\phi\Delta}^2}{m_\Delta^2 - m_\phi^2}\tilde{m}_{\phi\Delta}^2, \quad (3.2a)$$

$$M_2^2 \simeq m_\phi^2 - \frac{m_{\phi\Delta}^4}{m_\Delta^2 - m_\phi^2} + \tilde{m}_\phi^2 + 2\frac{m_{\phi\Delta}^2}{m_\Delta^2 - m_\phi^2}\tilde{m}_{\phi\Delta}^2, \quad (3.2b)$$

$$M_3^2 \simeq m_\Delta^2 + 2\frac{m_{\phi\Delta}^2}{m_\Delta^2 - m_\phi^2}\tilde{m}_{\phi\Delta}^2, \quad (3.2c)$$

$$M_4^2 \simeq m_\Delta^2 - 2\frac{m_{\phi\Delta}^2}{m_\Delta^2 - m_\phi^2}\tilde{m}_{\phi\Delta}^2, \quad (3.2d)$$

where

$$m_\Delta^2 \equiv \mu_\Delta^2 + (\lambda_{H\Delta 1} - \lambda_{H\Delta 2})\frac{v_H^2}{2}, \quad (3.3)$$

$$m_\phi^2 \equiv \mu_\phi^2 + \lambda_{H\phi}\frac{v_H^2}{2}, \quad \tilde{m}_\phi^2 \equiv -2\tilde{\mu}_\phi^2 - \tilde{\lambda}_{H\phi}v_H^2, \quad m_{\phi\Delta}^2 \equiv -\lambda_{H\Delta\phi}\frac{v_H^2}{2} \quad \text{and} \quad \tilde{m}_{\phi\Delta}^2 \equiv -\tilde{\lambda}_{H\Delta\phi}\frac{v_H^2}{2}.$$

For simplicity, we have assumed $m_\Delta^2 - m_\phi^2 \gg m_{\phi\Delta}^2$ as well as $m_\Delta^2 > m_\phi^2$. Notice also that $m_\phi^2 \gg \tilde{m}_\phi^2$ and $m_{\phi\Delta}^2 \gg \tilde{m}_{\phi\Delta}^2$, as the parameters indicated by tilde are the $U(1)_X$ -breaking ones. Thus, the pair of states (δ_1, δ_2) and (δ_3, δ_4) are nearly degenerate with $M_2^2 - M_1^2 - 2\tilde{m}_\phi^2 \simeq M_3^2 - M_4^2 \simeq 4m_{\phi\Delta}^2\tilde{m}_{\phi\Delta}^2/(m_\Delta^2 - m_\phi^2)$. We define the mass splitting

$$\delta \equiv M_2 - M_1 = \frac{M_2^2 - M_1^2}{M_1 + M_2}. \quad (3.4)$$

The mass eigenstates are

$$\begin{pmatrix} \delta_1 \\ \delta_2 \\ \delta_3 \\ \delta_4 \end{pmatrix} = \begin{pmatrix} \cos \alpha_1 & 0 & \sin \alpha_1 & 0 \\ 0 & \cos \alpha_2 & 0 & \sin \alpha_2 \\ -\sin \alpha_1 & 0 & \cos \alpha_1 & 0 \\ 0 & -\sin \alpha_2 & 0 & \cos \alpha_2 \end{pmatrix} \begin{pmatrix} \phi_1 \\ \phi_2 \\ \Delta_1 \\ \Delta_2 \end{pmatrix}, \quad (3.5)$$

where, at leading order, $|\tan 2\alpha_1| \simeq |\tan 2\alpha_2| \simeq 2m_{\phi\Delta}^2/(m_\Delta^2 - m_\phi^2)$. The difference in $|\alpha_1|$ and $|\alpha_2|$ is suppressed by the $U(1)_X$ -breaking terms. Notice that, if the couplings $\tilde{\lambda}_{H\phi}$ and $\tilde{\lambda}_{H\Delta\phi}$ were taken to be negative, the roles of δ_1 and δ_2 as well as those of δ_3 and δ_4 would be interchanged, with δ_2 being the lightest particle and the dark matter candidate. In appendix A, we describe in detail the mass matrix and give the general mass eigenvalues of the scalars and the mixing between $(\phi_1, \phi_2, \Delta_1, \Delta_2)$ with the mass eigenstates $(\delta_1, \delta_2, \delta_3, \delta_4)$. By taking μ_Δ^2 relatively large, the components of the triplet can be sufficiently heavy and the bounds from direct searches can be therefore avoided. In our model, the values of M_1

and M_2 are considered free parameters and can range from a few keV (in order to avoid too hot dark matter) to above the electroweak breaking scale.

For light scalar masses with $M_1 + M_2 < m_Z$, there will be an additional invisible decay mode of the Z boson into $\delta_1 \delta_2$ due to the coupling of Δ to the Z boson

$$\frac{i g_{\text{SU}(2)} \sin \alpha_1 \sin \alpha_2}{\cos \theta_W} [\delta_2 \partial_\mu \delta_1 - \delta_1 \partial_\mu \delta_2] Z^\mu, \quad (3.6)$$

where $g_{\text{SU}(2)}$ is the SM weak gauge coupling and θ_W is the Weinberg angle. The corresponding decay width is given by

$$\Gamma(Z \rightarrow \delta_1 \delta_2) = \frac{G_F \sin^2 \alpha_1 \sin^2 \alpha_2}{6\sqrt{2}\pi} m_Z^3, \quad (3.7)$$

which is strongly sensitive to the mixing between ϕ and Δ , *i.e.* $\sin \alpha_1 \sin \alpha_2$. δ_2 eventually decays into δ_1 and neutrinos via Z or $R - R'$ exchange as it is given in Eq. (5.17). The whole process appears as a Z invisible decay mode. Hence the present bound on the invisible decay width [12] constrains the mixing $\sin \alpha_1 \sin \alpha_2$ as

$$\Gamma(Z \rightarrow \delta_1 \delta_2) < 0.3\% \Gamma_{\text{invisible}} \Rightarrow \sin \alpha_1 \sin \alpha_2 < 0.07. \quad (3.8)$$

For heavier masses, this bound does not apply and larger mixing is in principle allowed.

For definiteness in the following study we will take the following typical values for the scalar parameters, unless otherwise indicated:

$$M_1 \simeq M_2 = 70 \text{ GeV}, \quad M_3 \simeq M_4 \simeq m_\Delta = 500 \text{ GeV}, \quad \delta = 50 \text{ MeV}, \\ \sin \alpha_1 \simeq -\sin \alpha_2 = -0.1. \quad (3.9)$$

In principle, in our model, the DM particle can have much smaller masses if strong fine-tuning is allowed in the masses (see Eq. (A.4a)). In this case, the lower bound on the mass is given by large scale structure formation, *i.e.* few keV (see *e.g.* [13]), and by big bang nucleosynthesis, depending on the dominant DM couplings to SM particles [14]. We do not consider further this case in our study and we focus only on electroweak-scale DM masses.

4. Lepton Sector

4.1 Neutrino Masses

Neutrino masses are protected by the symmetry of the model. If $U(1)_R \times U(1)_\phi \times U(1)_\Delta \times U(1)_\ell$ is conserved, neutrinos cannot possess a Majorana mass term. The unbroken \mathbb{Z}_2 symmetry prevents a Dirac mass term such as $R^\dagger \ell_{L\alpha}$. The term in $\mathcal{L}_{\ell_L \phi}$ is allowed by $U(1)_X$ but does not generate a neutrino mass term as neither ϕ nor Δ acquire a vacuum expectation value, $\langle \phi \rangle = \langle \Delta \rangle = 0$. We notice that if either of $U(1)_{L1}$, $U(1)_{L2}$ or $U(1)_{L3}$ (defined in Tab. 2) were conserved, the neutrino mass would be protected by a lepton number symmetry. Once the symmetry is explicitly broken, a Majorana mass term can emerge. We therefore expect the neutrino mass to depend on combinations $\tilde{g}_\Delta g \tilde{\lambda}_{H\Delta\phi}$, $\tilde{g}_\Delta g \tilde{\lambda}_{H\Delta\phi}$,

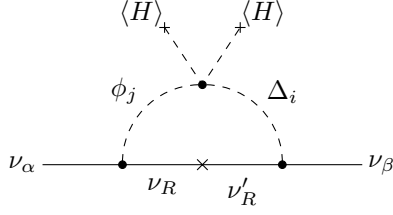


Figure 1: Effective neutrino mass generation at one loop.

$\tilde{g}_\Delta \tilde{g} \lambda_{H\Delta\phi}$ and $\tilde{g}_\Delta \tilde{g} \lambda_{H\Delta\phi}$. Thus, the smallness of neutrino masses can be explained by t'Hooft's criterion [15].

More specifically, an effective neutrino mass term,

$$-\mathcal{L}_{\nu_L\nu_L} = \frac{1}{2} (m_\nu)_{\alpha\beta} (\nu_L^T)_\alpha C (\nu_L)_\beta + \text{h.c.} , \quad (4.1)$$

arises at one loop-level [4, 1, 2, 3] through the diagram shown in Fig. 1. The neutrino mass matrix is given by

$$(m_\nu)_{\alpha\beta} = [g_\alpha(\tilde{g}_\Delta)_\beta + g_\beta(\tilde{g}_\Delta)_\alpha]\tilde{\eta} + [\tilde{g}_\alpha(\tilde{g}_\Delta)_\beta + \tilde{g}_\beta(\tilde{g}_\Delta)_\alpha]\eta , \quad (4.2)$$

and depends on \tilde{g}_Δ as expected. The determinant of the neutrino mass matrix vanishes, so one of the mass eigenvalues is zero, unless more vector-like fermionic doublets or copies of ϕ or Δ are added. In other words, within the present model with only one generation of R and R' fields, the neutrino mass spectrum is either normal hierarchical or inverted hierarchical. The terms η and $\tilde{\eta}$ can be explicitly computed

$$\eta = \frac{m_{RR}}{64\pi^2} \left(\frac{M_3^2}{m_{RR}^2 - M_3^2} \ln \frac{m_{RR}^2}{M_3^2} - \frac{M_1^2}{m_{RR}^2 - M_1^2} \ln \frac{m_{RR}^2}{M_1^2} \right) \sin 2\alpha_1 - [(\alpha_1, M_1^2, M_3^2) \rightarrow (\alpha_2, M_2^2, M_4^2)] , \quad (4.3a)$$

$$\tilde{\eta} = \frac{m_{RR}}{64\pi^2} \left(\frac{M_3^2}{m_{RR}^2 - M_3^2} \ln \frac{m_{RR}^2}{M_3^2} - \frac{M_1^2}{m_{RR}^2 - M_1^2} \ln \frac{m_{RR}^2}{M_1^2} \right) \sin 2\alpha_1 + [(\alpha_1, M_1^2, M_3^2) \rightarrow (\alpha_2, M_2^2, M_4^2)] . \quad (4.3b)$$

It is straightforward to check that in the limit in which $\lambda_{H\Delta\phi}$ and $\tilde{\lambda}_{H\Delta\phi}$ both vanish, *i.e.* $m_{\phi\Delta}^2 = \tilde{m}_{\phi\Delta}^2 = 0$, the neutrino mass becomes zero. This is expected as in this case the symmetry $U(1)_{L3}$ is exact (see Tab. 1 for definition) and no Majorana mass for neutrinos is allowed. In the limit of nearly-exact $U(1)_X$ symmetry, we have $M_1^2 \simeq M_2^2 \simeq m_\phi^2 - m_{\phi\Delta}^4/m_\Delta^2$,

$M_3^2 \simeq M_4^2$ and $\sin \alpha_1 \simeq -\sin \alpha_2$. As a result, in this limit we can approximately write

$$\eta \simeq \frac{m_{RR}}{16\pi^2} \frac{m_{\phi\Delta}^2}{m_\Delta^2 - m_\phi^2} \left(\frac{M_1^2}{m_{RR}^2 - M_1^2} \ln \frac{m_{RR}^2}{M_1^2} - \frac{m_\Delta^2}{m_{RR}^2 - m_\Delta^2} \ln \frac{m_{RR}^2}{m_\Delta^2} \right), \quad (4.4a)$$

$$\simeq -\frac{m_{RR}}{16\pi^2} \frac{m_{\phi\Delta}^2}{m_{RR}^2 - m_\Delta^2} \ln \frac{m_{RR}^2}{m_\Delta^2}, \quad (4.4b)$$

$$\begin{aligned} \tilde{\eta} \simeq & \frac{m_{RR}}{16\pi^2} \frac{\tilde{m}_\phi^2}{m_{RR}^2 - M_1^2} \frac{m_{\phi\Delta}^2}{m_\Delta^2 - m_\phi^2} \left(1 + \frac{(m_{RR}^2 - M_1^2)m_\Delta^2}{(m_{RR}^2 - m_\Delta^2)(m_\Delta^2 - m_\phi^2)} \ln \frac{m_{RR}^2}{m_\Delta^2} \right. \\ & \left. - \left(\frac{m_{RR}^2}{m_{RR}^2 - M_1^2} + \frac{M_1^2}{m_\Delta^2 - m_\phi^2} \right) \ln \frac{m_{RR}^2}{M_1^2} \right) \\ & + \frac{m_{RR}}{16\pi^2} \frac{\tilde{m}_{\phi\Delta}^2}{m_\Delta^2 - m_\phi^2} \left(\frac{M_1^2}{m_{RR}^2 - M_1^2} \ln \frac{m_{RR}^2}{M_1^2} - \frac{m_\Delta^2}{m_{RR}^2 - m_\Delta^2} \ln \frac{m_{RR}^2}{m_\Delta^2} \right), \end{aligned} \quad (4.4c)$$

$$\simeq \frac{m_{RR}}{16\pi^2} \left(\frac{\tilde{m}_\phi^2 m_{\phi\Delta}^2}{m_{RR}^2 m_\Delta^2} \left(\frac{m_{RR}^2}{m_{RR}^2 - m_\Delta^2} \ln \frac{m_{RR}^2}{m_\Delta^2} + 1 - \ln \frac{m_{RR}^2}{M_1^2} \right) - \frac{\tilde{m}_{\phi\Delta}^2}{m_{RR}^2 - m_\Delta^2} \ln \frac{m_{RR}^2}{m_\Delta^2} \right). \quad (4.4d)$$

We have expanded to first order in the $U(1)_X$ -breaking parameters and assumed that $m_{\phi\Delta}^2 \ll m_\Delta^2 - m_\phi^2$. In Eqs. (4.4b) and (4.4d), we have taken the limit $m_\phi^2, M_1^2 \ll m_\Delta^2, m_{RR}^2$ in addition. Notice that $\tilde{\eta}$ is suppressed by $U(1)_X$ -violating parameters $\tilde{m}_{\phi\Delta}^2/(m_{RR}^2 - m_\Delta^2)$ and $\tilde{m}_\phi^2/m_{RR}^2$ relative to η . On the other hand, the contribution of η to the neutrino mass is suppressed by the $U(1)_X$ -violating coupling $\tilde{g} \ll g$. As expected, the neutrino mass depends on the mixing between ϕ and Δ (given by the terms $\lambda_{H\Delta\phi}$ and $\tilde{\lambda}_{H\Delta\phi}$ after electroweak symmetry breaking) and on the coupling between the new sector with the leptonic doublet (*i.e.*, g, \tilde{g} and \tilde{g}_Δ). We can obtain an order of magnitude estimate for the couplings

$$g\tilde{g}_\Delta \simeq 3.4 \times 10^{-6} \frac{m_\nu}{0.05 \text{ eV}} \frac{70 \text{ GeV}}{M_1} \frac{50 \text{ MeV}}{\delta} \frac{m_{RR}}{300 \text{ GeV}} \frac{0.1}{|\sin \alpha_1|} \left(\frac{m_{RR}^2}{m_{RR}^2 - m_\Delta^2} \ln \frac{m_{RR}^2}{m_\Delta^2} + 1 - \ln \frac{m_{RR}^2}{M_1^2} \right)^{-1} \quad \text{for } 2\tilde{m}_\phi^2 m_{\phi\Delta}^2 / m_\Delta^2 \simeq 2M_1 \delta |\sin \alpha_1| \gg \tilde{m}_{\phi\Delta}^2, \quad (4.5a)$$

$$g\tilde{g}_\Delta \simeq 3.3 \times 10^{-6} \frac{m_\nu}{0.05 \text{ eV}} \frac{300 \text{ GeV}}{m_{RR}} \frac{1 \text{ GeV}^2}{\tilde{m}_{\phi\Delta}^2} \left(\frac{m_\Delta}{500 \text{ GeV}} \right)^2 \frac{m_{RR}^2 - m_\Delta^2}{m_\Delta^2} \left(\ln \frac{m_{RR}^2}{m_\Delta^2} \right)^{-1} \quad \text{for } 2\tilde{m}_\phi^2 m_{\phi\Delta}^2 / m_\Delta^2 \simeq 2M_1 \delta |\sin \alpha_1| \ll \tilde{m}_{\phi\Delta}^2, \quad (4.5b)$$

$$\tilde{g}\tilde{g}_\Delta \simeq 1.3 \times 10^{-10} \frac{m_\nu}{0.05 \text{ eV}} \frac{300 \text{ GeV}}{m_{RR}} \frac{0.1}{|\sin \alpha_1|} \frac{m_{RR}^2 - m_\Delta^2}{m_\Delta^2} \left(\ln \frac{m_{RR}^2}{m_\Delta^2} \right)^{-1}, \quad (4.6)$$

where we have taken as typical values $m_{RR} = 300 \text{ GeV}$ and $m_\nu = 0.05 \text{ eV}$ in Eqs. (4.4b) and (4.4d). We will use these values in the remaining analysis unless otherwise explained. We remind that we have $\tilde{m}_{\phi\Delta}^2 \lesssim M_1 \delta / \sin \alpha_1$.

4.2 Lepton Flavour Violating Rare Decays

Besides the neutrino mass measurements, the leptonic sector is already constrained from searches of LFV rare decay. In this specific model, the LFV couplings in Eqs. (2.5b) and (2.7) lead to LFV rare decays of charged leptons $\ell_\alpha \rightarrow \ell_\beta \gamma$. They are induced by similar loop diagrams as the one leading to neutrino masses. Using the general result for one loop LFV rare decays [16], we find for the decay width

$$\Gamma(\ell_\alpha \rightarrow \ell_\beta \gamma) \simeq \frac{\alpha m_{\ell_\alpha}^5}{(768\pi^2 m_{RR}^2)^2} X_{\alpha\beta} , \quad (4.7)$$

with $X_{\alpha\beta}$ defined by

$$\begin{aligned} X_{\alpha\beta} = & |(g_\alpha + \tilde{g}_\alpha)^*(g_\beta + \tilde{g}_\beta)(\cos^2 \alpha_1 H(m_{RR}^2/M_1^2) + \sin^2 \alpha_1 H(m_{RR}^2/M_3^2) \\ & + (g_\alpha - \tilde{g}_\alpha)^*(g_\beta - \tilde{g}_\beta)(\cos^2 \alpha_2 H(m_{RR}^2/M_2^2) + \sin^2 \alpha_2 H(m_{RR}^2/M_4^2) \\ & + (\tilde{g}_\Delta)_\alpha^*(\tilde{g}_\Delta)_\beta (2K(m_{RR}^2/m_{\Delta^{++}}^2) - 2H(m_{RR}^2/m_{\Delta^{++}}^2) + K(m_{RR}^2/m_{\Delta^+}^2)/2)|^2 , \end{aligned} \quad (4.8)$$

where

$$H(t) = \frac{t(2 + 3t - 6t^2 + t^3 + 6t \ln t)}{(t-1)^4} \quad \text{and} \quad K(t) = 2t \left[\frac{2t^2 + 5t - 1}{(t-1)^3} - \frac{6t^2 \ln t}{(t-1)^4} \right] . \quad (4.9)$$

The corresponding branching ratios are calculated to be

$$\text{Br}(\mu \rightarrow e \gamma) \approx 2.5 \times 10^{-9} \left(\frac{300 \text{ GeV}}{m_{RR}} \right)^4 \left| \frac{g_\mu^*}{0.1} \frac{g_e}{0.1} \right|^2 \quad \text{and} \quad (4.10a)$$

$$\text{Br}(\tau \rightarrow \alpha \gamma) \approx 4.5 \times 10^{-10} \left(\frac{300 \text{ GeV}}{m_{RR}} \right)^4 \left| \frac{g_\tau^*}{0.1} \frac{g_\alpha}{0.1} \right|^2 , \quad (4.10b)$$

where we have neglected the contributions from the suppressed $U(1)_X$ -breaking couplings. LFV rare decays are already strongly constrained by several measurements [12] to

$$\text{Br}(\mu \rightarrow e \gamma) < 1.2 \times 10^{-11} \quad (4.11a)$$

$$\text{Br}(\tau \rightarrow e \gamma) < 1.1 \times 10^{-7} \quad (4.11b)$$

$$\text{Br}(\tau \rightarrow \mu \gamma) < 6.8 \times 10^{-8} . \quad (4.11c)$$

The MEG experiment aims at improving on the present bound down to $\text{Br}(\mu \rightarrow e \gamma) \sim 10^{-13}$ and has released the first result last year, $\text{Br}(\mu \rightarrow e \gamma) < 2.8 \times 10^{-11}$ at 90% C.L. [17]. The bounds on the LFV τ decays will be further improved by a Super-B factory [18].

Inserting the values for the couplings in Eq. (4.7), we find that the bounds on $\text{Br}(\tau \rightarrow e \gamma)$ and $\text{Br}(\tau \rightarrow \mu \gamma)$ can be readily satisfied even for values of m_{RR} as small as 100 GeV and $g_{\mu,\tau}$ as large as 0.2. For $g_e, g_\mu \sim 0.1$, the bound on $\text{Br}(\mu \rightarrow e \gamma)$ points towards relatively large values of m_{RR} , $m_{RR} \gtrsim 1.1$ TeV. However, taking $g_\mu \sim 0.02$ and $g_e \sim 0.01$, m_{RR} as small as 100 GeV can still be compatible with the present bound on $\mu \rightarrow e \gamma$. Notice that, for such values, the expression for neutrino masses, Eq. (4.5a), implies $\tilde{g}_\Delta \sim 0.01g$ so despite relatively small g , the hierarchy imposed by the approximate $U(1)_X$ symmetry (i.e., $\tilde{g}_\Delta \ll g$) is still satisfied. An alternative possibility is $g_e \ll g_\mu$ or $g_e \gg g_\mu$. In the

case $g_e \ll g_\mu$, the $e\alpha$ elements of the neutrino mass matrix should be accounted for by the $\tilde{g}\tilde{g}_\Delta\eta$ contribution; *i.e.*, $(m_\nu)_{e\alpha} = [\tilde{g}_e(\tilde{g}_\Delta)_\alpha + \tilde{g}_\alpha(\tilde{g}_\Delta)_e]\eta$. Similar consideration holds also for the case $g_e \gg g_\mu$.

Since the processes $\mu \rightarrow eee$ and $\mu \rightarrow e$ conversion on nuclei cannot proceed at tree level in this model, the contributions in both cases are one-loop effects and are dominated by the effective vertex $\bar{\mu}\sigma^{\mu\nu}P_L e F_{\mu\nu}$. The bound on this effective coupling from $\mu \rightarrow e\gamma$ is stronger than those from $\mu \rightarrow eee$ and $\mu \rightarrow e$ conversion [19] because the former is a two body decay.

4.3 Anomalous Magnetic Moment of the Muon

Similarly to the LFV rare decay, the new couplings in Eqs. (2.5b) and (2.7) give rise to magnetic dipole moments of charged leptons ℓ_α

$$a_\alpha = \frac{(g-2)_\alpha}{2} = \frac{m_{\ell_\alpha}^2}{192\pi^2 m_{RR}^2} X_{\alpha\alpha}, \quad (4.12)$$

where $X_{\alpha\alpha}$ is defined in Eq. (4.8). This contribution leads to a deviation of the dipole moment of the muon from the SM prediction

$$\delta a_\mu = \delta(g-2)_\mu/2 \simeq \frac{m_\mu^2}{192\pi^2 m_{RR}^2} |g_\mu|^2 \sim 2.4 \times 10^{-12} \left(\frac{300 \text{ GeV}}{m_{RR}} \right)^2 \left| \frac{g_\mu}{0.1} \right|^2, \quad (4.13)$$

where we have neglected the $U(1)_X$ -breaking couplings. The present uncertainty on a_μ is 6×10^{-10} [12] so the deviation is below the current experimental sensitivity and theoretical uncertainty. After an improvement on the theoretical and experimental uncertainties, the muon anomalous magnetic dipole moment, δa_μ , will be a powerful test of this model.

5. Dark Matter

As discussed in sec. 2, the lightest neutral scalar, δ_1 , is stable due to the \mathbb{Z}_2 symmetry and is a candidate for the dark matter of the Universe. In order to be thermally produced in the Early Universe with the right abundance, the annihilation cross section needs to be

$$\langle \sigma(\delta_1\delta_1 \rightarrow \text{anything})v \rangle \simeq 3 \times 10^{-26} \text{ cm}^3/\text{sec}, \quad (5.1)$$

where v is the relative velocity. More precisely, as the mass splitting between the lightest and next-to-lightest scalar particles might be small, we have to take into account both particles during freeze-out. This requires a calculation of the self annihilation cross section of both δ_1 and δ_2 as well as the coannihilation cross section of δ_1 - δ_2 . δ_2 then decays into δ_1 , so the number of DM particles today is equal to the sum of the numbers of δ_1 and δ_2 at the decoupling. In the following, we shall discuss these modes and determine the range of the parameters for which each mode will be relevant. We shall then discuss the possibility of direct and indirect detection of dark matter within the present model.

5.1 Dark Matter Abundance in the Universe

Several processes contribute to the annihilation of dark matter in the Early Universe. They are depicted in Fig. 2. Their relative importance depends on the choice of parameters of the model. For the typical values of masses and the couplings that we consider, the dominant annihilation modes determining the dark matter abundance are mediated by the Higgs and the remaining modes are negligible.

Higgs-mediated annihilation: An important annihilation channel is the annihilation via Higgs exchange. From Eqs. (2.3) and (2.5), we find that the coupling of $\delta_{1,2}$ to the Higgs field is given by

$$\begin{aligned} \lambda_L v_H h \delta_i^2 &\equiv \frac{v_H}{2} \left((\lambda_{H\Delta 1} - \lambda_{H\Delta 2}) \sin^2 \alpha_1 + \lambda_{H\phi} \cos^2 \alpha_1 - 2\lambda_{H\Delta\phi} \sin \alpha_1 \cos \alpha_1 \right) h \delta_i^2 \\ &= \frac{\left(M_1^2 - \mu_\phi^2 \cos^2 \alpha_1 - \mu_\Delta^2 \sin^2 \alpha_1 \right)}{v_H} h \delta_i^2 \end{aligned} \quad (5.2)$$

with $i = 1, 2$. For simplicity we neglect the subdominant $U(1)_X$ -violating terms. The $\delta_1 \delta_2 h$ coupling is absent in the CP conserving Higgs potential. The CP violating terms lead to a coupling $\delta_1 \delta_2 h$ and therefore induces coannihilations, which suppress the DM relic density.

At low values of masses, $M_1 \ll m_W$, with m_W the W -boson mass, the annihilation into fermion pair final states is important. The cross section for this channel [20] is given by

$$\langle \sigma(\delta_1 \delta_1 \rightarrow f \bar{f})_{Hv} \rangle = N_c \frac{|\lambda_L|^2}{\pi} \frac{m_f^2}{(4M_1^2 - m_h^2)^2} \frac{(M_1^2 - m_f^2)^{3/2}}{M_1^3}, \quad (5.3)$$

where m_f is the fermion mass for the kinematically accessible channels and $N_c = 3$ (1) for quarks (leptons). In the limit $\delta \ll 2M_1$, we have to take into account the annihilation of $\delta_2 \delta_2$ in the calculation of the DM abundance as

$$\langle \sigma(\delta_2 \delta_2 \rightarrow f \bar{f})_{Hv} \rangle \simeq \langle \sigma(\delta_1 \delta_1 \rightarrow f \bar{f})_{Hv} \rangle.$$

For $M_1 > m_{b,\tau}$, the Higgs-mediated modes can dominate the freeze-out processes. For light dark matter, $M_1 < m_\tau$, they can annihilate only into light fermions so the cross section is suppressed by the small fermion masses and cannot provide the dominant annihilation channel at freeze-out.

For heavier masses, $M_1 \gtrsim m_W$, three-body decays and decays into gauge bosons need to be taken into account. As shown in [21], even for $70 \text{ GeV} \lesssim M_1 < m_W$, the three body annihilation mode $\delta_1 \delta_1 \rightarrow h^* \rightarrow WW^* \rightarrow W f \bar{f}'$ is comparable to or can even dominate over $\delta_1 \delta_1 \rightarrow \bar{f} f$. For $M_1 > m_W$, the Higgs-mediated DM annihilation into a W boson pair becomes kinematically allowed and soon dominates. Its annihilation cross section is given by

$$\begin{aligned} \langle \sigma(\delta_1 \delta_1 \rightarrow WW)v \rangle_H &= \frac{g_{SU(2)}^4 |\lambda_L|^2}{32\pi M_1^2} \left(\frac{v_H^2}{4M_1^2 - m_h^2} \right)^2 \sqrt{1 - \frac{m_W^2}{M_1^2}} \\ &\quad \left(2 - \frac{M_1^2}{m_W^2} \left(1 - \sqrt{1 - \frac{m_W^2}{M_1^2}} \right)^2 \right)^2. \end{aligned} \quad (5.4)$$

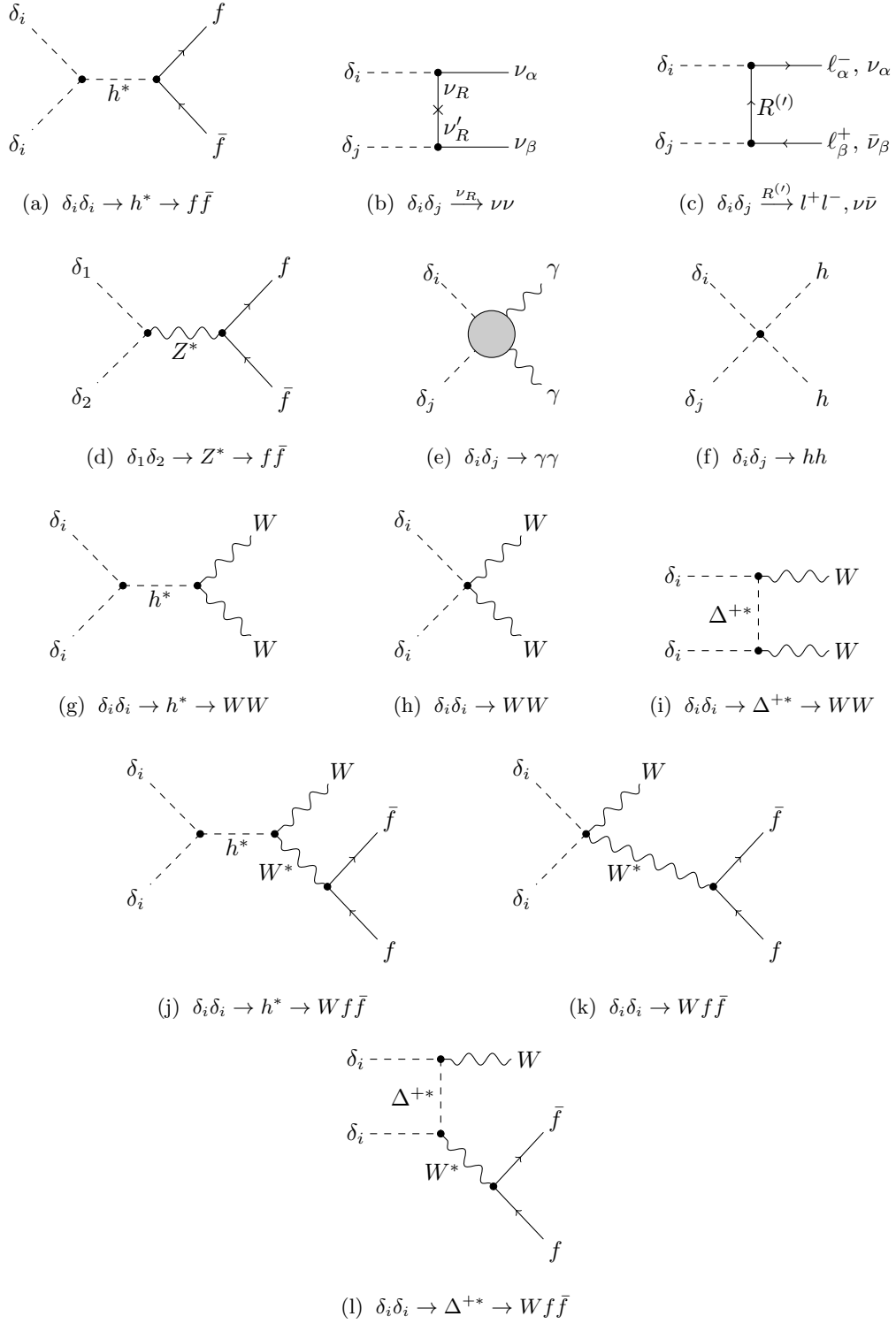


Figure 2: Different dark matter pair annihilation channels.

As the mass increases, more channels such as annihilation into Z boson pairs and top pairs become available but, the annihilation into a W boson pair will still dominate the cross section. Regardless of the final states, the cross section of any annihilation mode through s -channel Higgs exchange can be related to the corresponding Higgs decay rate by

$$\langle \sigma(\delta_1 \delta_1 \rightarrow h^* \rightarrow \text{final state})_{Hv} \rangle = (2m_h \Gamma(h \rightarrow \text{final state}))|_{m_h \rightarrow 2M_1} \frac{1}{4M_1^2} \frac{4|\lambda_L|^2 v_H^2}{(4M_1^2 - m_h^2)^2}. \quad (5.5)$$

Hence the importance of each channel can be obtained from the branching ratio of the corresponding Higgs decay channel by identifying the Higgs mass with the centre of mass energy $E_{\text{CM}} = 2M_1$. Let us take our typical value $M_1 = 70$ GeV to evaluate λ_L . In this case, according to HDecay [22], the Higgs decay width is $\Gamma|_{2M_1} = 8.3$ MeV. Taking into account the contribution of δ_2 for $\delta \ll M_1$, for $m_h = 120$ GeV, the dark matter abundance implies a Higgs-DM coupling of $\lambda_L \approx 0.07$. We will use this value for reference in this study, unless otherwise indicated. As it can be seen from Eq. (5.5), larger Higgs masses m_h require a larger Higgs-DM coupling λ_L .

Annihilation via gauge interactions: Another possibly relevant contribution is due to gauge interactions, which in principle involves two different processes. The process shown in Fig. 2(i) is suppressed by the heavy mass of Δ^+ , but, for $M_1 > m_W$, the one shown in Fig. 2(h) results in the cross section

$$\langle \sigma(\delta_1 \delta_1 \rightarrow WW)v \rangle_g = \frac{g_{SU(2)}^4}{32\pi M_1^2} \sin^2 \alpha_1 \sin^2 \alpha_2 \sqrt{1 - \frac{m_W^2}{M_1^2}} \left(2 - \frac{M_1^2}{m_W^2} \left(1 - \sqrt{1 - \frac{m_W^2}{M_1^2}} \right)^2 \right)^2. \quad (5.6)$$

A comparison with the Higgs-mediated annihilation into W boson pairs shows that the annihilation via gauge interactions is subdominant for small mixing in the neutral sector as can be seen by computing the following ratio of cross sections

$$\frac{\langle \sigma(\delta_1 \delta_1 \rightarrow WW)v \rangle_H}{\langle \sigma(\delta_1 \delta_1 \rightarrow WW)v \rangle_g} = \frac{|\lambda_L|^2}{\sin^2 \alpha_1 \sin^2 \alpha_2} \left(\frac{v_H^2}{4M_1^2 - m_h^2} \right)^2. \quad (5.7)$$

This cross section can lead to the correct DM abundance for large mixing in the scalar sector, allowed for $M_1 > m_Z/2$, and typical masses in the range $M_1 \simeq 100$ GeV – 200 GeV. We do not consider this possibility further. The three body final state annihilation processes, see Fig. 2(k), are related in a similar way. If the annihilation via gauge interaction dominates, the box diagram with two W bosons can be significant in the DM nucleon interaction and therefore in the direct DM detection experiments.

Annihilation into Higgs pair: For $M_1 > m_h$, the annihilation into a Higgs pair can take place and even dominate over other channels. In particular, the quartic couplings of H , Φ and Δ can lead to

$$\langle \sigma(\delta_1 \delta_1 \rightarrow hh)v \rangle \simeq \frac{|\lambda_L|^2 (M_1^2 - m_h^2)^{1/2}}{16\pi M_1^3}. \quad (5.8)$$

For simplicity, in the following we consider only the region $M_1 < m_h$, where this annihilation channel is absent.

Annihilation into neutrino and anti-neutrino pairs: A dark matter pair can annihilate into pairs of (anti-)neutrinos through the t -channel chirality-flipping diagram shown in Fig. 2(b). To leading order in $U(1)_X$ -violating couplings, the cross section is given by

$$\langle \sigma(\delta_i \delta_j \rightarrow \nu_\alpha \nu_\beta) v \rangle = \langle \sigma(\delta_i \delta_j \rightarrow \bar{\nu}_\alpha \bar{\nu}_\beta) v \rangle = \frac{\sin^2 2\alpha_1}{32\pi(1 + \delta_{\alpha\beta})m_{RR}^2} |g_\alpha(\tilde{g}_\Delta)_\beta + g_\beta(\tilde{g}_\Delta)_\alpha|^2 \quad (5.9)$$

with $i, j = 1, 2$ in the limit $M_1^2 \ll m_{RR}^2$.

For typical values, the cross section can be estimated to be

$$\begin{aligned} \langle \sigma(\delta_i \delta_j \rightarrow \nu_\alpha \nu_\beta) v \rangle &\sim 2 \times 10^{-37} \left(\frac{300 \text{ GeV}}{m_{RR}} \right)^2 \left(\frac{\sin^2 2\alpha_1}{0.04} \right) \left(\frac{\tilde{g}_\Delta}{10^{-5}} \right)^2 \left(\frac{g}{0.1} \right)^2 \frac{\text{cm}^3}{\text{sec}} \\ &\ll \langle \sigma(\delta_1 \delta_1 \rightarrow \text{anything}) v \rangle \end{aligned} \quad (5.10)$$

and it cannot therefore explain the DM abundance.

A quantitative connection between neutrino masses and the dark matter abundance [2] can be obtained if a different appropriate choice for the $U(1)$ symmetry, protecting neutrino masses, is made. In this case the dominant dark matter annihilation channel can be $\delta_1 \delta_1 \rightarrow \nu\nu, \bar{\nu}\bar{\nu}$. This leads to an upper bound of the order of 300 GeV on the masses of E_R^- , $E_R'^+$, ν_R and ν_R' making their production at the LHC possible.

Annihilation into lepton pairs via heavy fermion exchange: In addition, processes such as $\delta_i \delta_j \rightarrow l^- l^+, \nu \bar{\nu}$ can also take place via heavy-fermion exchange, which is shown in Fig. 2(c). The cross section can be written as

$$\left\langle \sigma(\delta_i \delta_j \rightarrow \ell_\alpha^- \ell_\beta^+, \nu_\alpha \bar{\nu}_\beta) v \right\rangle \simeq \frac{\cos^2 \alpha_i \cos^2 \alpha_j |g_\alpha g_\beta|^2}{32\pi} \frac{(m_\alpha^2 + m_\beta^2)}{(M_i M_j + m_{RR}^2)^2} \frac{(M_i + M_j)^2}{M_i M_j}, \quad (5.11)$$

to leading order in the final state lepton masses. The p -wave contribution vanishes. The estimate for the dominant annihilation into τ leptons with our typical values results in

$$\langle \sigma(\delta_i \delta_j \rightarrow \tau^- \tau^+) v \rangle \simeq 3.3 \times 10^{-32} \left| \frac{g_\tau}{0.1} \right|^4 \frac{(70^2 + 300^2)^2 \text{GeV}^4}{(M_i M_j + m_{RR}^2)^2} \frac{\text{cm}^3}{\text{sec}}, \quad (5.12)$$

which cannot give a dominant contribution to the dark matter abundance. Note that this cross section depends on some of the parameters which control neutrino masses and the rate of LFV processes and cannot therefore be enhanced arbitrarily by a different choice of parameters.

DM annihilation into photons: There are several one-loop diagrams that contribute to annihilation into a photon pair, as summarised in Fig. 2(e). For the values of M_1 up to the electroweak scale, the cross section can be estimated as

$$\langle \sigma(\delta_1 \delta_1 \rightarrow \gamma\gamma) v \rangle \sim \frac{\alpha^2 G_F^2 \sin^4 \alpha_1}{4\pi^3} M_1^2 \sim 3 \times 10^{-34} \left(\frac{\sin \alpha_1}{0.1} \right)^4 \left(\frac{M_1}{70 \text{ GeV}} \right)^2 \frac{\text{cm}^3}{\text{sec}}, \quad (5.13)$$

which is negligible.

Coannihilations of δ_1 and δ_2 via the Z boson: Through the mixing with the neutral components of the triplet Δ , δ_1 and δ_2 couple also to the Z boson (see Eq. (3.6)). This coupling allows the $\delta_1\delta_2$ coannihilation into kinematically allowed modes, such as $\nu\bar{\nu}$, e^-e^+ depending on the values of M_1 and M_2 , shown in Fig. 2(d). The cross section can be evaluated as

$$\langle\sigma(\delta_1\delta_2 \rightarrow f\bar{f})v\rangle = N_c \frac{G_F^2 \sin^2 \alpha_1 \sin^2 \alpha_2}{2\pi} \left[\frac{m_f^2 \sqrt{M_1^2 - m_f^2} \delta^2}{M_1^3} + \frac{32(a_L^2 + a_R^2)(M_1 v)^2}{3 \left(1 - 4 \frac{M_1^2}{m_Z^2}\right)^2} \right], \quad (5.14)$$

where $a_L^2 + a_R^2$ is given by

$$\frac{1}{4} \cos^2 2\theta_W + \sin^4 \theta_W, \quad \frac{1}{4}, \quad \frac{1}{36} (9 - 4 \cos 2\theta_W + 4 \cos 4\theta_W), \quad \frac{1}{36} (6 + 2 \cos 2\theta_W + \cos 4\theta_W), \quad (5.15)$$

for leptons, neutrinos, up-type quarks and down-type quarks. Hence $a_L^2 + a_R^2 \approx 0.13 - 0.25$.

If the mass of the dark matter is larger than that of the b quark but smaller than m_Z , this mode of annihilation can be estimated for our typical values in Eq. (3.9) to be

$$\langle\sigma(\delta_1\delta_2 \rightarrow b\bar{b})v\rangle \simeq \left(\frac{\sin \alpha_1 \sin \alpha_2}{0.01} \right)^2 \left(7 \times 10^{-37} \frac{\delta^2}{(50 \text{ MeV})^2} + 4 \times 10^{-28} v^2 \right) \frac{\text{cm}^3}{\text{sec}}, \quad (5.16)$$

where the p -wave contribution dominates over the s -wave for typical value of $v \sim \sqrt{1/20}$ at the DM decoupling time. For our typical values, this is only about $\lesssim 1\%$ of the total annihilation channel cross section ($\delta_i\delta_i \rightarrow \text{anything}$). Unless $|\sin \alpha_i| > 0.5$, we expect coannihilations not to significantly modify the amount of dark matter at freeze-out with respect to the case in which they are neglected. Notice that in the case of $M_1 \simeq m_Z/2$, there is an enhancement of the coannihilation cross section, which can contribute significantly to freeze out.

δ_2 decay: δ_2 eventually decays into δ_1 and neutrinos or other kinematically allowed light fermions via Z exchange. It can also decay into lepton-pairs via the $R - R'$ exchange. To leading order in the $U(1)_X$ -breaking couplings and the mass splitting δ , the decay rates are

$$\Gamma(\delta_2 \xrightarrow{R} \delta_1 \nu \nu) = \Gamma(\delta_2 \xrightarrow{R} \delta_1 \bar{\nu} \bar{\nu}) \simeq \frac{\delta^5 \sin^2 2\alpha_1}{1920(1 + \delta_{\alpha\beta})\pi^3 M_1^2 m_{RR}^2} |g_\alpha \tilde{g}_{\Delta\beta} + g_\beta \tilde{g}_{\Delta\alpha}|^2, \quad (5.17a)$$

$$\Gamma(\delta_2 \xrightarrow{Z} \delta_1 \nu \bar{\nu}) \simeq \frac{G_F^2 \delta^5}{15\pi^3} \sin^4 \alpha_1. \quad (5.17b)$$

For $\delta \gg m_e$, the decay rate into electron final state pairs is

$$\begin{aligned} \Gamma(\delta_2 \xrightarrow{Z} \delta_1 e^+ e^-) &\simeq 4(a_L^2 + a_R^d) \Gamma(\delta_2 \xrightarrow{Z} \delta_1 \nu \bar{\nu}) = (\cos^2 2\theta_W + 4 \sin^4 \theta_W) \Gamma(\delta_2 \xrightarrow{Z} \delta_1 \nu \bar{\nu}) \\ &\simeq \frac{G_F^2 \delta^5}{30\pi^3} \sin^4 \alpha_1. \end{aligned} \quad (5.18)$$

This channel is suppressed with respect to the corresponding neutrino channel by a factor of 2. The same decay mediated via the new heavy fermions has a rate given by

$$\Gamma(\delta_2 \xrightarrow{R} \delta_1 e^+ e^-, \delta_1 \nu \bar{\nu}) \simeq \frac{|g_\alpha g_\beta|^2 \cos^2 \alpha_1 \cos^2 \alpha_2 \delta^5}{480 \pi^3 (M_1^2 - m_{RR}^2)^2}. \quad (5.19)$$

For the typical values we have chosen for the scalar and leptonic parameters, the decay via the Z boson into a neutrino anti-neutrino pair dominates with a decay width

$$\Gamma \approx 14 \left(\frac{\delta}{50 \text{ MeV}} \right)^5 \left(\frac{\sin \alpha_1}{0.1} \right)^4 \text{ sec}^{-1}. \quad (5.20)$$

Hence, the decay happens before big bang nucleosynthesis (BBN) and does not affect the BBN predictions. We comment on the case with a small mass splitting $\delta \sim \mathcal{O}(10 - 100) \text{ keV}$, as it is required in the low mass region to explain DAMA via inelastic scattering, in the next section.

5.2 Direct Dark Matter Searches

Direct DM searches look for interactions of DM with the nuclei (electrons) in the detector. The differential scattering rate is given by (see *e.g.* [23])

$$\frac{dR}{dE_R}(E_R, t) = \frac{\rho_\chi}{2M_1 m_r^2} [f_p/f_n Z + (A - Z)]^2 \sigma_n F^2(E_R) \int_{v_{min}}^{v_{esc}} d^3v \frac{f_{local}(\vec{v}, t)}{v}, \quad (5.21)$$

where E_R is the recoil energy of the nucleus, ρ_χ is the local DM density, M_1 is the DM mass, m_r is the reduced mass of the dark matter-nucleus system; v is the speed of dark matter relative to the nucleus; f_p/f_n is the ratio of the coupling of DM to protons compared to neutrons, $F(E_R)$ is a nuclear form factor describing the nuclear structure, f_{local} is the local DM velocity distribution, v_{esc} is the escape velocity and finally σ_n is the dark matter–neutron cross section.

σ_n and f_p/f_n depend on the dominant DM-nucleon interaction which can be obtained by rotating the diagrams in Fig. 2(a) and Fig. 2(d). There is also a contribution from two W boson exchange box diagram, which is negligible for our typical values, but becomes important above the W boson mass threshold and large values of $\sin \alpha_1$. The t -channel Higgs boson exchange leads to [20]

$$\sigma_n = \frac{|\lambda_L|^2}{\pi} \frac{\mu_{\delta_1 n}^2 m_p^2}{M_1^2 m_h^4} f^2 \approx 5.2 \times 10^{-44} \left(\frac{\lambda_L}{0.07} \right)^2 \left(\frac{70 \text{ GeV}}{M_1} \right)^2 \left(\frac{120 \text{ GeV}}{m_h} \right)^4 \left(\frac{f}{0.3} \right)^2 \text{ cm}^2, \quad (5.22)$$

with $f_p/f_n \approx 1$. Here $\mu_{\delta_1 n}$ is the reduced mass of the dark matter-neutron system, m_p is the nucleon mass and f parametrises the nuclear matrix element, $0.14 < f < 0.66$ in [20]. Note that the Higgs-mediated cross section strongly depends on the uncertainties in the nuclear matrix element. This interaction would lead to elastic spin-independent (eSI) scattering and to nuclear recoils which have been extensively searched for by various experiments.

If the mass splitting between δ_1 and δ_2 is small ($\mathcal{O}(10 - 100) \text{ keV}$), $\delta_1 n \rightarrow \delta_2 n$ through t -channel Z boson exchange becomes kinematically allowed. In the limit $\delta \ll \mu_{\delta_1 n}$, the

cross section is given by

$$\sigma_n = \frac{8}{\pi} \sin^2 \alpha_1 \sin^2 \alpha_2 G_F^2 \mu_{\delta_1 n}^2 \approx 1.3 \times 10^{-41} \left(\frac{\sin \alpha_1 \sin \alpha_2}{0.01} \right)^2 \text{ cm}^2, \quad (5.23)$$

with $f_p/f_n = -(1 - 4 \sin^2 \theta_W) \approx -0.08$. The dependence on δ is reflected in the lower limit of the integral in Eq. (5.21). This accommodates the inelastic spin-independent (iSI) scattering scenario, in which dark matter, δ_1 , is converted into a slightly heavier particle, δ_2 , while scattering off nuclei [24] (see also [25, 26]). It should be pointed out that our model accommodates the small mass splittings required, $\delta \sim (\tilde{m}_\phi^2 + \sin \alpha_1 \tilde{m}_{\phi\Delta}^2)/M_1$, as it is naturally suppressed by the $U(1)_X$ -breaking terms.

Experimental constraints:: In the following, we discuss the experimental constraints from direct searches ¹. Many experiments have searched for nuclear recoil signals, *e.g.* XENON10 [29], ZEPLIN-III [30], CRESST-II [31], KIMS [32] as well as PICASSO [33], and, recently, the CDMS II [6], the CoGeNT [8] and the XENON100 [9] experiments. The most stringent bounds on the spin-independent elastic cross section come from CDMS-II and XENON100: for $M_1 = 55 \text{ GeV}$ $\sigma_n < 3.4 \times 10^{-44} \text{ cm}^2$ at 90% C.L. from the XENON100 first data and for $M_1 = 70 \text{ GeV}$ $\sigma_n < 3.8 \times 10^{-44} \text{ cm}^2$ from CDMS-II. Evidence and hints of dark matter detection have also been reported but await further confirmation. The DAMA/LIBRA experiment in Gran Sasso searches for an annual modulation of the DM scattering signal due to the Earth orbit around the Sun and the consequently annual change in the DM velocity relative to the detector. It has been reporting a positive signal for 13 years [7]. The effect which is seen by DAMA at 8.2σ is refuted by other experiments attempting to directly detect the dark matter. The CDMS-II experiment reported two candidate events requiring a 1σ -allowed region in the $M_1 - \sigma_n$ plane roughly between $21 \text{ GeV} \lesssim M_1 \lesssim 51 \text{ GeV}$ and $\sigma_n \simeq 10^{-44} \text{ cm}^2 - 10^{-43} \text{ cm}^2$ for eSI scattering being consistent with all other null results. The allowed values of σ_n extend up to $\sigma_n \sim 10^{-41} \text{ cm}^2$ for low masses if the bounds from XENON100 can be relaxed [9]. The CoGeNT experiment sees an excess of events at very low energies below 3 keV, which, if not due to backgrounds, can be interpreted as dark matter-nucleon eSI scattering with $M_1 \sim 7 \text{ GeV} - 11 \text{ GeV}$ and $\sigma_N \sim 3 \times 10^{-41} \text{ cm}^2 - 1 \times 10^{-40} \text{ cm}^2$ (for other analysis of this and other DM direct searches data, see also Refs. [34, 35]). These results can be compatible with the DAMA preferred region for an intermediate amount of channelling but are in tension with the XENON and CDMS results. Recent analyses of the relevant experiments have been performed [34] (see also [35, 36]) in order to obtain global limits on the DM-nucleon cross section and indicate a tension between DAMA, CDMS, XENON100 and CoGeNT data. However, the results still depend strongly on the underlying assumptions of the experiments, which are not settled yet. For example, a different choice for the effective light yield of the XENON100 [9, 11] or the channelling in the DAMA experiment can lead to significantly different allowed region of parameter space. Taking a conservative effective light yield for the XENON experiment,

¹The proposed explanation of the DAMA signal by scattering off atomic electrons [27] is disfavoured by different analysis due to the tension between the DAMA spectral data and the modulated signal [26, 28] as well as the loop induced interactions with nuclei [28].

the combination of Fig. 2 in [34] and Fig. 3 in [20] (also in Fig. 2 in [35] and Fig. 5 of [36]) suggests that there might remain a region of parameter space ~ 10 GeV explaining DAMA or CoGeNT by eSI scattering via Higgs exchange which is compatible with the bounds from other experiments. However, this region is excluded if the effective light yield of XENON100 is higher or the region allowed by DAMA is more restricted. The cross section required by DAMA and CoGeNT needs an intermediate amount of channelling and/or a sizable source of background at low energy in CoGeNT. A stronger tension between the regions preferred by DAMA and CoGeNT with the one required to explain the two CDMS events remains and could be partially alleviated only by assuming a different DM velocity distribution (see *e.g.* [35]). We do not therefore restrict ourselves to one analysis but base our discussion on the analyses in [37, 38] and [34, 35, 36].

Elastic DM-nucleon scattering: The DM-nucleon cross-section in Eq. (5.22) is controlled by the same parameters as the dominant annihilation cross section, Eq. (5.5). After factoring out λ_L , we find

$$\sigma_n(\simeq \sigma_p) = \frac{f^2 \mu_{\delta_1 n}^2 m_p^2 (4M_1^2 - m_h^2)^2 \langle \sigma(\delta_1 \delta_1 \rightarrow h^* \rightarrow \text{SM final states}) v \rangle}{\pi M_1 m_h^4 v_H^2 4\Gamma(h \rightarrow \text{SM final states})|_{m_h \rightarrow 2M_1}}. \quad (5.24)$$

Thus, once the DM mass is fixed, the DM-nucleon cross section is uniquely determined and depends mildly on the value of the Higgs mass. Ignoring the positive signal in favour of DM scattering, the recent analysis leads to a typical cross section $\sigma_n \lesssim 2 - 3 \times 10^{-44} \text{cm}^2$ for a DM mass of $\sim 10 - 130$ GeV. These values can be accommodated in our model, depending on the value of the Higgs, DM mass and the nuclear matrix element. We expect soon a positive signal in direct detection experiments unless $M_1 \simeq m_h/2$ (see Eq. (5.24)). At $M_1 \sim 70$ GeV, CDMS and XENON100 are already constraining the parameter space and large values of f , $f \gtrsim 0.2$, are not compatible with the bounds from direct DM detection experiments. For smaller values of the mass, the elastic cross section is suppressed by the cancellation between the Higgs mass and $2M_1$, see Eq. (5.24). For example, for a slightly smaller DM mass, *e.g.* $M_1 = 65$ GeV, the corresponding total Higgs decay width $\Gamma = 5$ MeV leads to $\lambda_L \approx 0.04$ and therefore a value of the cross section $\sigma_n \approx 1.8 \times 10^{-44} \text{cm}^2$ for $f = 0.3$ which is below present bounds.

If DM has been observed and the two candidate events of CDMS-II are due to dark matter, the allowed region in the parameter space, $M_1 \sim 20 - 50$ GeV and $\sigma_n \sim 10^{-44} \text{cm}^2 - 10^{-43} \text{cm}^2$, can be accommodated within our model via scattering by Higgs exchange with *e.g.* $M_1 = 50$ GeV and a light Higgs $m_h = 120$ GeV, and $\sigma_n \simeq 5.4 \times 10^{-44} \text{cm}^2$, where we have used the lower bound on $f = 0.14$. In the case of sizable coannihilations, the required DM coannihilation cross section is smaller and therefore the elastic DM - nucleon cross section is reduced. This improves the consistency with the two candidate events of CDMS-II. The recent CoGeNT results, if interpreted as a dark matter signal, require a different region in the parameter space, with smaller masses $7 \text{ GeV} \lesssim M_1 \lesssim 11 \text{ GeV}$ and higher cross sections $\sigma_n \sim 10^{-41} \text{cm}^2 - 10^{-40} \text{cm}^2$, which might also explain DAMA for intermediate channelling, as discussed above. In our model, for fixed M_1 in the range of

interest we predict the value of the cross section

$$\sigma_n \approx 1.3 \times 10^{-40} \left(\frac{f}{0.3} \right)^2 \left(\frac{8 \text{ GeV}}{M_1} \right)^2 \text{ cm}^2, \quad (5.25)$$

in agreement with the experimental results for small M_1 and larger f . It is curious to notice that this is exactly the range where eSI solution with channelling for DAMA comes close to the preliminary XENON100 bounds [9]. On the other hand as shown in [10], in this range the bounds are sensitive to astrophysical uncertainties such as the dark matter escape velocity. In future, more robust bounds might conclusively refute this solution for DAMA. In this case, our model is still compatible, as M_1 can take on higher values.

Inelastic dark matter: The inelastic SI scenario has recently attracted much interest as it can simultaneously accommodate the DAMA signal and the CDMS data [6] because scattering off heavy nuclei (such as ^{127}I) is favoured with respect to the one onto light nuclei and the modulated signal is enhanced compared to the unmodulated one. The latest global analysis [34] finds three possible regions for $M_1 = 10 \text{ GeV}$, 40 GeV , 50 GeV . However, the regions around $M_1 = 40 \text{ GeV}$, 50 GeV are both excluded by the CRESST-II data as discussed in [34] and by the bound of Super-Kamiokande on the neutrino flux from DM annihilations in the Sun [39]. We will focus on the lowest allowed values of the cross section in the region around $M_1 = 10 \text{ GeV}$: $\sigma_p \sim 1 \times 10^{-40} \text{ cm}^2$, which roughly corresponds to $\sigma_n = 3.3 \times 10^{-40} \text{ cm}^2$. This region is also suggested by [38]. The DM-neutron cross section can be estimated from Eq. (5.23) as $\sigma_n \approx 6 \times 10^{-40} (\sin \alpha_1 \sin \alpha_2 / 0.07)^2 \text{ cm}^2$, where we have used the largest allowed value of $\sin \alpha_1$, close to the present bound from the invisible Z -decay and testable with a moderate improvement of these searches.

A comparison with Fig. 7 of [38] shows that the resulting cross section can still explain DAMA, whereas the analysis [34] already excludes this cross section assuming a standard DM profile. In general, iSI scattering strongly depends on the velocity distribution because only the high energy tail can scatter. Hence, this region is probably still allowed due to the astrophysical uncertainties. Concerning the values of masses, it requires fine tuning at the % level to obtain a light DM mass M_1 in the region of interest. As already mentioned, the mass splitting $\delta \sim 20 \text{ keV}$ is naturally small due to the $U(1)_X$ symmetry and could be obtained for example for $\tilde{m}_\phi^2, \tilde{m}_{\phi\Delta}^2 \sin \alpha_1 \sim 2 \times 10^{-4} \text{ GeV}^2$. In this case neutrino masses would be dominated by the contribution due to $\tilde{g}\tilde{g}_\Delta\eta$, as $\tilde{\eta}(\tilde{m}_\phi^2, \tilde{m}_{\phi\Delta}^2)$ is too small. For a small mass splitting, $\delta \sim \mathcal{O}(10 - 100) \text{ keV}$, as it is required in the low mass region to explain DAMA, the decay of δ_2 , which survives after freeze-out, happens at very late times and after galaxies have formed, as $\tau_{\delta_2} \sim 7 \times 10^{15} (20 \text{ keV}/\delta)^5 (0.07/\sin \alpha_1 \sin \alpha_2)^2 \text{ s}$. Its effect can be estimated by looking at the energy densities $\rho_\nu^f = \rho_\nu^i + \rho_2 - \rho_1$, ρ_i denoting the energy density of δ_i . Since δ_i are non-relativistic, the energy densities are given by $\rho_i = n_i M_i$. The decay leads to a negligible energy density increase for neutrinos

$$\frac{\Delta \rho_\nu}{\rho_\nu} \equiv \frac{\rho_\nu^f - \rho_\nu^i}{\rho_\nu} = \frac{\Omega_2 - \Omega_1}{\Omega_\nu} \approx \frac{\delta}{2M_1} \frac{\Omega_{\text{DM}}}{\Omega_\nu} \lesssim 1.2 \times 10^{-4}, \quad (5.26)$$

where $\Omega_\nu \gtrsim \sqrt{\Delta m_{atm}^2}/91.5 \text{ eV} \approx 5 \times 10^{-4}$ has been used as lower bound for Ω_ν . As their energy is too small $E_\nu \leq \delta \sim 20 \text{ keV}$, they evade detection in neutrino detectors and,

since the energy of neutrinos is below the nuclear binding energy, they cannot destroy the outcome of big bang nucleosynthesis.

Notice that, in addition to the iSI scattering, elastic scattering will necessarily be induced with a cross section determined by M_1 as discussed above. We expect a large cross section for elastic scattering in addition to the inelastic one, which can be compatible with present bounds from CDMS and XENON10 for small values of f and/or a conservative treatment of experimental uncertainties [40] and astrophysical parameters [10].

If the mass splitting δ is even smaller, the exothermic dark matter (exoDM) [41] scenario might explain DAMA and the other direct detection experiments within our model.

In summary, present direct dark matter experiments provide contradictory results, with DAMA showing a strong evidence of annual modulation of the signal, CDMS and CoGeNT showing possible hints in favour of DM if their signal is not due to backgrounds, and the other experiments reporting null results in the region of the parameter space of interest. If we dismiss the possible positive signals found so far, our model typically predicts an elastic cross section within the reach of present and future experiments, unless $M_1 \rightarrow m_h/2$. Otherwise, if we take the positive signals as a direct observation of dark matter, various possible explanation can be accommodated in our model, depending on the values of the parameters. For $M_1 \sim (21 - 51)$ GeV we can explain the CDMS two-events, while DAMA, with intermediate channelling, and CoGeNT require much smaller masses, $M_1 \sim (7 - 11)$ GeV, and a correspondingly higher cross section. The latter signals can also be explained with the iSI scattering which requires a value of $\sin \alpha_1$ close to the upper bound, $\sin^2 \alpha_1 \simeq 0.07$, and therefore testable in the future in invisible Z -decay searches. In the near future, new results for direct DM search are expected and in particular further data from XENON100 experiment [42] and CRESST will help to clarify these issues.

5.3 Indirect Dark Matter Searches

Indirect dark matter searches look for gamma-rays, neutrinos, positrons, anti-protons and anti-deuterons from the regions of the galaxy or astrophysical objects (in the case of neutrinos) where the concentration of dark matter is expected to be relatively high and annihilations are therefore strongly enhanced. A study in Ref. [43] has recently derived limits on the different dark matter annihilation channels leading to electron positron production by studying radio and gamma ray from galactic center. Moreover, in Ref. [44] bounds on different DM annihilation modes have been derived from Fermi-LAT diffuse gamma ray data. A comparison of the different annihilation channels with Fig. 2 of [44] shows that our model is not constrained by the Fermi-LAT data but a future improvement on the sensitivity will be able to provide useful constraints for light $\mathcal{O}(\text{few GeV})$ dark matter masses, when the dominant annihilation is into light quarks or τ s. The coannihilation of DM into photons at one loop which has been estimated in Eq. (5.13) is well below the current bounds from EGRET and Fermi-LAT [45], too. The anti-deuteron cosmic ray search experiments AMS-02 and GAPS can test the DM annihilation to hadronic final states in the region around $\mathcal{O}(100 \text{ GeV})$ [46].

Dark matter can also be captured in compact objects such as the Earth and the Sun due to the scattering on nuclei. This leads to a large flux of neutrinos either prompt

from the annihilations or as subsequent decay products from annihilations into charged leptons and quarks. This feature can be tested in present and future neutrino detectors such as SuperKamiokande and IceCube. These detectors will measure the total neutrino flux and can in principle determine the neutrino spectrum, if a sufficient energy resolution is available [47]. Notice that, although the overall detection threshold of IceCube is rather high, its DeepCore component has a threshold of 10 GeV [48] and can be used for this purpose, if $M_1 > 10$ GeV. If the nucleon-dark matter interaction, as well as the dark matter annihilation, dominantly proceed via Higgs-exchange, the effect can be significant. In this case, for masses below 70 GeV, the dominant annihilation channel is into b -quarks as the cross section scales with the final fermion mass squared. We therefore expect a rather soft neutrino spectrum with a fixed branching ratio into c -quarks and τ s, below present constraints [49]. For heavier masses new channels are open: annihilations into gauge and Higgs bosons lead to a hard neutrino spectrum which can be more easily detected at present and future detectors [50, 51]. In the iSI case, with a mass splitting in the $\mathcal{O}(10 - 100)$ keV region, due to the high inelastic scattering cross section, dark matter would be copiously captured in the Sun [39, 52, 51]. A population of δ_2 particles would form, which could subsequently decay into δ_1 along with low energy neutrinos, not detectable with present techniques, or could annihilate as discussed above. For the inelastic scattering cross sections and required DM mass M_1 (see the previous section), the hard channels, as annihilations into τ s and into neutrinos, are already constrained by Super-Kamiokande data to give a subdominant contribution, but annihilations into b s and c s are allowed [39]. We recall that in our model, the main annihilation modes are $\delta_1\delta_1 \rightarrow h^* \rightarrow b\bar{b}$ and $\delta_2\delta_2 \rightarrow h^* \rightarrow b\bar{b}$ giving a rather soft neutrino spectrum. Therefore, it is possible to explain DAMA with inelastic dark matter evading the present constraints from dark matter neutrino searches from the Sun.

6. Other Constraints on the Model and Laboratory Signatures

In this section we discuss electroweak precision observables which might constrain the model further and speculate about possible collider signatures.

6.1 Electroweak Precision Tests

As the additional particles are close to the electroweak scale and are charged under the SM gauge group, they lead to corrections to the electroweak precision parameters [53, 54, 55]. It has been pointed out in [55] that all contributions of physics coupling only to the lepton sector can be condensed into seven effective oblique parameters. The dominant effects are contained in the quantities \hat{S} , \hat{T} , W , Y [54, 55].

A study of an additional vector-like lepton doublet [56] shows that the contributions to \hat{S} and \hat{T} parameter exactly cancel out, because R and R' have equal masses, while W and Y receive tiny corrections

$$W = \frac{g_{\text{SU}(2)}^2}{120\pi^2} \frac{m_W^2}{m_{RR}^2} \quad \text{and} \quad Y = \frac{g_{\text{U}(1)}^2}{120\pi^2} \frac{m_W^2}{m_{RR}^2} ,$$

respectively.

We can neglect the contribution of ϕ to the electroweak precision parameters because it is suppressed by a factor of $|\sin \alpha_1 \sin \alpha_2|$ relative to that of Δ . For the latter, the direct calculation of the wave function renormalisation results in

$$\hat{S} = \frac{g_{\text{SU}(2)}^2}{24\pi^2} \xi, \quad \hat{T} = \frac{25 g_{\text{SU}(2)}^2}{576\pi^2} \frac{m_\Delta^2}{m_W^2} \xi^2, \quad W = -\frac{7 g_{\text{SU}(2)}^2}{720\pi^2} \frac{m_W^2}{m_\Delta^2}, \quad Y = -\frac{7 g_{\text{U}(1)}^2}{480\pi^2} \frac{m_W^2}{m_\Delta^2}, \quad (6.1)$$

where the relation $2 m_{\Delta+}^2 = m_\Delta^2 + m_{\Delta++}^2$ has been used and the results have been expanded in

$$\xi \equiv \frac{m_{\Delta++}^2 - m_\Delta^2}{m_\Delta^2} = \lambda_{H\Delta 2} \frac{v_H^2}{m_\Delta^2}. \quad (6.2)$$

It can be easily seen that the two additional fermionic doublets with opposite hypercharge as well as the triplet without VEV have a well defined decoupling limit. ξ can be chosen such that it cancels the contribution from the SM Higgs, relaxing the upper bound from the electroweak precision data on the Higgs mass. Without cancellation (*i.e.*, for a light Higgs mass), the \hat{T} parameter constrains $\xi \lesssim 0.1$ which translates into a bound on the splitting of the components of the triplet. This results in a mild bound on $\lambda_{H\Delta 2}$, *e.g.*, for $m_\Delta \simeq 500$ GeV, the bound is $\lambda_{H\Delta 2} \lesssim 0.5$. The other electroweak precision constraints are readily satisfied.

6.2 Signatures at Colliders

Higgs Boson Searches: If $M_1 < m_h/2$, the coupling which is responsible for the DM annihilation also leads to the decay of the SM Higgs boson into DM particles. For $\lambda_L \gtrsim m_b/v_H$, its branching ratio becomes significant and even dominates over the decay into $b\bar{b}$. This happens for our typical parameter set, where we have $\lambda_L \simeq 0.07$. Hence, a light ($m_h < 2m_W$) SM Higgs decays dominantly into $\delta_1\delta_1$ or $\delta_2\delta_2$. The DM particles δ_1 escape the detector. In case that the mass splitting between δ_2 and δ_1 is less than twice the electron mass, δ_2 will decay only into δ_1 and neutrinos which are also invisible. For larger mass splittings, the δ_2 decay into e^-e^+ can lead to a displaced vertex, which opens a new and distinct channel for discovering the Higgs [57], provided that the decay takes place inside the detector. For this to happen, the diameter of the detector, d , bounds the decay width Γ_{δ_2} by $d\Gamma_{\delta_2}/2\gamma \gtrsim v$ with v being the velocity of the particle δ_2 and $\gamma = (1 - v^2)^{-1/2}$. Assuming a dominant decay via the Z boson, this translates into a bound on the mass splitting δ

$$\delta^5 \sin^4 \alpha_1 \gtrsim 60\pi^3 \frac{\gamma v}{G_F^2 d}. \quad (6.3)$$

Hence, for the maximally allowed mixing $\sin^2 \alpha_1 \simeq 0.07$ in the case of $M_1 + M_2 < m_Z$, the ATLAS Muon detector [58] with a diameter of 22 m already requires a mass splitting of $\delta \gtrsim 480 \text{ MeV}(\gamma v)^{1/5}$. This displaced vertex would be a clear signal for a neutral next-to-lightest particle with SM couplings.

Prospects for the LHC: Since this model contains several particles with masses in the reach of the LHC, we expect a rich phenomenology within the upcoming years. If the

new particles are not too heavy, the charged particles Δ^{++} , Δ^+ , E_R^- and $E_R'^+$ as well as the neutral particles δ_3 , δ_4 , ν_R and ν_R' can be produced through electroweak interactions. They will then decay into the SM particles plus δ_1 or δ_2 . At the LHC, δ_1 appears as a missing energy signal. δ_2 subsequently decays into $\delta_1\nu\bar{\nu}$ or, if kinematically possible, into $\delta_1 e^- e^+$. If the decay happens outside the detector or is into neutrinos, the displaced vertex cannot be observed and this decay will contribute to the missing energy signal. Since the masses of the components of the electroweak triplet Δ fulfil the relation

$$2m_{\Delta^+}^2 = m_{\Delta^{++}}^2 + m_{\Delta^-}^2,$$

it might be discovered by measuring the masses of Δ^+ , Δ^{++} and δ_3 at the LHC, as long as $\lambda_{H\Delta\phi}$ and $\tilde{\lambda}_{H\Delta\phi}$ are small $m_{\Delta} \simeq M_3 \simeq M_4$ (see Eq. (A.4)). In fact, from the electroweak precision data, Δ^+ and Δ^{++} are expected to be quasi-degenerate with a small mass splitting of $m_{\Delta^{++}}^2 - m_{\Delta^+}^2 = \lambda_{H\Delta 2} v_H^2/2$. The coupling g_{α} can be determined by measuring the decay modes of E_R^- because the branching ratio $\text{Br}(E_R^- \rightarrow \ell_{\alpha}^- \delta_{1,2}) \propto |g_{\alpha}|^2$. The values of the components of \tilde{g}_{Δ} can be derived from a study of the decay modes of Δ^+ and Δ^{++} . In particular, $\Gamma(\Delta^{++} \rightarrow \ell_{\alpha}^+ \ell_{\beta}^+ \delta_{1,2}) \propto |(\tilde{g}_{\Delta})_{\alpha} g_{\beta} + (\tilde{g}_{\Delta})_{\beta} g_{\alpha}|^2$. By directly extracting g and \tilde{g}_{Δ} at the LHC, it will be possible to cross-check the information on them from rare decays and the neutrino mass matrix (see sec. 4).

As discussed in sec. 3, an improvement of the uncertainty on the invisible decay width of Z can test the model for $M_1 < m_Z/2$. LHC, being a Z factory, can in principle improve the precision of the $\Gamma(Z \rightarrow \text{invisible})$ measurement.

7. Conclusions

In this paper, we have proposed a model that simultaneously explains the missing mass problem of the universe and the tiny neutrino masses. In addition to the SM particle content, there are only a complex scalar singlet and triplet as well as a vector-like electroweak fermionic doublet. We impose an approximate $U(1)_X$ symmetry which is broken to a remnant \mathbb{Z}_2 symmetry. The unbroken \mathbb{Z}_2 symmetry guarantees the stability of the lightest scalar in the model, δ_1 , a quasi-singlet of $SU(2)_L$, which plays the role of dark matter. In the limit of exact $U(1)_X$ symmetry, neutrinos are massless and only after the $U(1)_X$ is broken to the \mathbb{Z}_2 symmetry, neutrinos acquire a mass term at the one-loop level. The \mathbb{Z}_2 symmetry forbids a tree-level neutrino mass term and the usual seesaw mechanism does not take place. Hence, the smallness of neutrino masses is explained by the small breaking of the $U(1)_X$ symmetry as well as the loop suppression. With the minimal particle content of the model, one of the neutrino mass eigenvalues vanishes and the neutrino mass scheme is therefore hierarchical. In order to obtain a non-hierarchical neutrino mass scheme, the minimality of the model has to be relaxed and more vector-like fermionic doublets have to be added. The strongest constraints come from searches for lepton flavour violating processes, in particular $\mu \rightarrow e\gamma$, which already probes the relevant parameter space. Future searches for $\mu \rightarrow e\gamma$ will provide a very sensitive test of our model.

In this model, DM is produced thermally in the Early Universe. We discussed the different dark matter annihilation channels and identified the dominant one to be the one

via Higgs exchange, for $M_1 \ll m_W$. All other channels are subdominant. The predicted cross section is compatible with the value required to explain the observed DM abundance.

The interactions responsible for DM freeze-out induce also scattering of dark matter off nuclei, relevant for direct DM searches. For our typical values $M_1 = 70$ GeV, δ_1 scatters elastically via Higgs exchange. The obtained scattering cross section is just below the current experimental bound and moderate improvements on the sensitivity can probe part of the relevant parameter space. Our model can also accommodate light dark matter with mass in the few GeV range, which has been invoked to explain the CoGeNT and DAMA results via elastic scattering. This process is mediated by the Higgs exchange and can have the required value for the cross section. For heavier masses, $M_1 \sim 20$ –50 GeV, the two events recently reported by CDMS can be interpreted as dark matter elastic scattering with a cross section which is compatible with the predictions of our model. The first results of the XENON100 experiment [9] disfavour most of the parameter region of DAMA, CoGeNT and the two events from CDMS depending on the assumptions on astrophysical uncertainties [10] and the ratio between electron equivalent energy and nuclear recoil energy \mathcal{L}_{eff} [11]. Further data from the XENON100 experiment as well as other experiments is needed to resolve this uncertainty. We also studied the possibility of inelastic spin independent solution for DAMA. For small mass splittings and small dark matter masses, δ_1 can scatter inelastically to δ_2 via Z boson exchange through mixing between scalar singlet and triplet. In our model the mass splitting δ can be naturally small due to the $U(1)_X$ symmetry. In order to accommodate the solution, the singlet-triplet mixing has to be relatively large and just below the upper bound from the invisible Z boson decay width. Thus, a slight improvement on the precision of the invisible Z decay width can probe this phenomenologically interesting part of the parameter space in our model.

We demonstrated that bounds on electroweak precision observables do not constrain the model further. Even more, the upper bound on the SM Higgs from electroweak precision data can be relaxed. The new particles can in principle be produced at the LHC and will eventually decay into stable δ_1 which escapes detection. The second lightest scalar, δ_2 , dominantly decays via Z exchange and might lead to a displaced vertex in the detector for sufficiently large mass splitting δ , or can decay outside the detector contributing to the missing energy signal. It is possible that $H \rightarrow \delta_1 \delta_1$ and $H \rightarrow \delta_2 \delta_2$ dominate over the SM mode $H \rightarrow b\bar{b}$, if $\delta_{1,2}$ are sufficiently light. In this case, the Higgs would decay mainly invisibly. The relevant coupling λ_L for this decay is fixed by the DM annihilation rate. Collider searches for the fermionic doublet can be also performed. By studying the subsequent decay of the charged components of the doublet into a charged lepton, we can determine the Yukawa couplings of these particles to different flavours. The flavour structure of these couplings also determines the flavour structure of the neutrino mass matrix so this provides another method to cross check the model.

Let us finally, comment on an alternative possibility, which leads to a tight connection between neutrino masses and the dark matter abundance [2]. If the guiding symmetry is not $U(1)_X$, but an approximate lepton number $U(1)_L$ or $U(1)_{B-L}$, the dominant dark matter annihilation channel may be $\delta_1 \delta_1 \rightarrow \nu_\alpha \nu_\beta, \bar{\nu}_\alpha \bar{\nu}_\beta$ resulting in a direct connection

between the dark matter abundance and neutrino masses. This leads to an upper bound of the order of 300 GeV on the masses of E_R^- , $E_R'^+$, ν_R and ν_R' guaranteeing their production at the LHC. In this case, the neutrino flux from dark matter annihilations inside the Sun will be monochromatic with a general flavour composition determined by the flavour structure of the new Yukawa couplings of the model. As recently shown in [59], this can lead to a novel seasonal variation in IceCube which cannot take place in models predicting only a continuous spectrum or democratic neutrino flavour composition.

In summary, we have presented here a model which explains simultaneously the origin of neutrino masses and the dark matter. A global $U(1)_X$ symmetry, explicitly broken to a residual \mathbb{Z}_2 guarantees the smallness of neutrino masses, generated at the loop- level, and the stability of dark matter. The model has a very rich phenomenology, such as lepton flavour violating processes, invisible decays of the Z -boson, collider signatures, which will make the model testable in the near future. Dark matter annihilations dominantly proceed via Higgs-exchange. Elastic and/or inelastic scattering off-nuclei can also be induced by the Higgs or Z exchange and can explain the possible signal or hints for dark matter direct detection which have been recently reported. So far, we have considered an explicit breaking of the additional $U(1)_X$ symmetry, but a version with a gauged $U(1)_X$ symmetry is in preparation.

Acknowledgements

The authors would like to thank C. Boehm for initial discussions and L. Lopez Honorez and C. Yaguna for useful discussions about the importance of processes with three-body final state for the DM abundance. Y.F. would like to acknowledge ICTP, where a part of this work was done for hospitality of its staff and the generous support. S.P. and M.S. would like to thank the PH-TH unit at CERN for hospitality and support during the initial stages of this study.

A. Scalar Mass Spectrum

The terms in Eqs. (2.3) and (2.6) with the vacuum expectation values defined in Eq. (3.1) lead to the following charged scalar masses

$$m_{\Delta^{++}}^2 = \mu_\Delta^2 + \frac{\lambda_{H\Delta 1} + \lambda_{H\Delta 2}}{2} v_H^2, \quad (\text{A.1a})$$

$$m_{\Delta^+}^2 = \mu_\Delta^2 + \frac{\lambda_{H\Delta 1}}{2} v_H^2. \quad (\text{A.1b})$$

In order to obtain the mass eigenvalues of the neutral scalars, one has to diagonalise their mass matrix. Remember that we have decomposed Δ^0 and ϕ as $\Delta^0 \equiv (\Delta_1 + i\Delta_2)/\sqrt{2}$ and $\phi \equiv (\phi_1 + i\phi_2)/\sqrt{2}$. In the basis $(\phi_1, \phi_2, \Delta_1, \Delta_2)$, the mass matrix is given by

$$m_s^2 = \begin{pmatrix} m_{\phi 1}^2 & 0 & m_{\phi\Delta}^2 + \tilde{m}_{\phi\Delta}^2 & 0 \\ \cdot & m_{\phi 2}^2 & 0 & -m_{\phi\Delta}^2 + \tilde{m}_{\phi\Delta}^2 \\ \cdot & \cdot & m_\Delta^2 & 0 \\ \cdot & \cdot & \cdot & m_\Delta^2 \end{pmatrix}, \quad (\text{A.2})$$

where

$$m_{\phi 1}^2 = \mu_\phi^2 + 2\tilde{\mu}_\phi^2 + \left(\lambda_{H\phi} + 2\tilde{\lambda}_{H\phi}\right) \frac{v_H^2}{2} \equiv m_\phi^2 - \tilde{m}_\phi^2, \quad (\text{A.3a})$$

$$m_{\phi 2}^2 = \mu_\phi^2 - 2\tilde{\mu}_\phi^2 + \left(\lambda_{H\phi} - 2\tilde{\lambda}_{H\phi}\right) \frac{v_H^2}{2} \equiv m_\phi^2 + \tilde{m}_\phi^2, \quad (\text{A.3b})$$

$$m_\Delta^2 = \mu_\Delta^2 + (\lambda_{H\Delta 1} - \lambda_{H\Delta 2}) \frac{v_H^2}{2}, \quad (\text{A.3c})$$

$$m_{\phi\Delta}^2 = -\lambda_{H\Delta\phi} \frac{v_H^2}{2}, \quad (\text{A.3d})$$

$$\tilde{m}_{\phi\Delta}^2 = -\tilde{\lambda}_{H\Delta\phi} \frac{v_H^2}{2}. \quad (\text{A.3e})$$

The diagonalisation by a transformation into the mass basis given in Eq. (3.5) yields the mass eigenvalues

$$M_1^2 = \frac{1}{2} \left(m_{\phi 1}^2 + m_\Delta^2 - \sqrt{(m_\Delta^2 - m_{\phi 1}^2)^2 + 4(m_{\phi\Delta}^2 + \tilde{m}_{\phi\Delta}^2)^2} \right) \simeq m_{\phi 1}^2 - \frac{(m_{\phi\Delta}^2 + \tilde{m}_{\phi\Delta}^2)^2}{m_\Delta^2 - m_{\phi 1}^2}, \quad (\text{A.4a})$$

$$M_2^2 = \frac{1}{2} \left(m_{\phi 2}^2 + m_\Delta^2 - \sqrt{(m_\Delta^2 - m_{\phi 2}^2)^2 + 4(m_{\phi\Delta}^2 - \tilde{m}_{\phi\Delta}^2)^2} \right) \simeq m_{\phi 2}^2 - \frac{(m_{\phi\Delta}^2 - \tilde{m}_{\phi\Delta}^2)^2}{m_\Delta^2 - m_{\phi 2}^2}, \quad (\text{A.4b})$$

$$M_3^2 = \frac{1}{2} \left(m_{\phi 1}^2 + m_\Delta^2 + \sqrt{(m_\Delta^2 - m_{\phi 1}^2)^2 + 4(m_{\phi\Delta}^2 + \tilde{m}_{\phi\Delta}^2)^2} \right) \simeq m_\Delta^2 + \frac{(m_{\phi\Delta}^2 + \tilde{m}_{\phi\Delta}^2)^2}{m_\Delta^2 - m_{\phi 1}^2}, \quad (\text{A.4c})$$

$$M_4^2 = \frac{1}{2} \left(m_{\phi 2}^2 + m_\Delta^2 + \sqrt{(m_\Delta^2 - m_{\phi 2}^2)^2 + 4(m_{\phi\Delta}^2 - \tilde{m}_{\phi\Delta}^2)^2} \right) \simeq m_\Delta^2 + \frac{(m_{\phi\Delta}^2 - \tilde{m}_{\phi\Delta}^2)^2}{m_\Delta^2 - m_{\phi 2}^2}, \quad (\text{A.4d})$$

where in the last equation, we have assumed

$$m_\Delta^2 > m_{\phi 2}^2, m_{\phi 1}^2 \text{ and } m_\Delta^2 - m_{\phi 1}^2, m_\Delta^2 - m_{\phi 2}^2 \gg m_{\phi\Delta}^2 \pm \tilde{m}_{\phi\Delta}^2.$$

Positiveness of M_i^2 guarantees $\langle\phi\rangle = \langle\Delta\rangle = 0$. The mixing angles are

$$\sin \alpha_1 \cos \alpha_1 = - \frac{m_{\phi\Delta}^2 + \tilde{m}_{\phi\Delta}^2}{\sqrt{(m_\Delta^2 - m_{\phi 1}^2)^2 + 4(m_{\phi\Delta}^2 + \tilde{m}_{\phi\Delta}^2)^2}}, \quad (\text{A.5a})$$

$$\sin \alpha_2 \cos \alpha_2 = \frac{m_{\phi\Delta}^2 - \tilde{m}_{\phi\Delta}^2}{\sqrt{(m_\Delta^2 - m_{\phi 2}^2)^2 + 4(m_{\phi\Delta}^2 - \tilde{m}_{\phi\Delta}^2)^2}}. \quad (\text{A.5b})$$

References

- [1] L. M. Krauss, S. Nasri, and M. Trodden, *A model for neutrino masses and dark matter*, Phys. Rev. **D67** (2003) 085002, [[hep-ph/0210389](#)].

- K. Cheung and O. Seto, *Phenomenology of TeV right-handed neutrino and the dark matter model*, Phys. Rev. **D69** (2004) 113009, [[hep-ph/0403003](#)].
- T. Asaka, S. Blanchet, and M. Shaposhnikov, *The nuMSM, dark matter and neutrino masses*, Phys. Lett. **B631** (2005) 151–156, [[hep-ph/0503065](#)].
- E. Ma, *Verifiable radiative seesaw mechanism of neutrino mass and dark matter*, Phys. Rev. **D73** (2006) 077301, [[hep-ph/0601225](#)].
- J. Kubo, E. Ma, and D. Suematsu, *Cold dark matter, radiative neutrino mass, $\mu\mu \rightarrow e\gamma$, and neutrinoless double beta decay*, Phys. Lett. **B642** (2006) 18–23, [[hep-ph/0604114](#)].
- E. J. Chun and H. B. Kim, *Axino Light Dark Matter and Neutrino Masses with R-parity Violation*, JHEP **10** (2006) 082, [[hep-ph/0607076](#)].
- T. Hambye, K. Kannike, E. Ma, and M. Raidal, *Emanations of Dark Matter: Muon Anomalous Magnetic Moment, Radiative Neutrino Mass, and Novel Leptogenesis at the TeV Scale*, Phys. Rev. **D75** (2007) 095003, [[hep-ph/0609228](#)].
- J. Kubo and D. Suematsu, *Neutrino masses and CDM in a non-supersymmetric model*, Phys. Lett. **B643** (2006) 336–341, [[hep-ph/0610006](#)].
- M. Aoki, S. Kanemura, and O. Seto, *Neutrino mass, Dark Matter and Baryon Asymmetry via TeV-Scale Physics without Fine-Tuning*, Phys. Rev. Lett. **102** (2009) 051805, [[arXiv:0807.0361](#)].
- M. Aoki, S. Kanemura, and O. Seto, *A Model of TeV Scale Physics for Neutrino Mass, Dark Matter and Baryon Asymmetry and its Phenomenology*, Phys. Rev. **D80** (2009) 033007, [[arXiv:0904.3829](#)].
- B. Bajc, T. Enkhbat, D. K. Ghosh, G. Senjanovic, and Y. Zhang, *MSSM in view of PAMELA and Fermi-LAT*, JHEP **05** (2010) 048, [[arXiv:1002.3631](#)].
- [2] C. Boehm, Y. Farzan, T. Hambye, S. Palomares-Ruiz, and S. Pascoli, *Are small neutrino masses unveiling the missing mass problem of the universe?*, Phys. Rev. **D77** (2008) 043516, [[hep-ph/0612228](#)].
- [3] Y. Farzan, *A minimal model linking two great mysteries: neutrino mass and dark matter*, Phys. Rev. **D80** (2009) 073009, [[arXiv:0908.3729](#)].
- [4] A. Zee, *A Theory of Lepton Number Violation, Neutrino Majorana Mass, and Oscillation*, Phys. Lett. **B93** (1980) 389.
- K. S. Babu, *Model of ‘Calculable’ Majorana Neutrino Masses*, Phys. Lett. **B203** (1988) 132.
- E. Ma, *Pathways to Naturally Small Neutrino Masses*, Phys. Rev. Lett. **81** (1998) 1171–1174, [[hep-ph/9805219](#)].
- [5] **WMAP** Collaboration, E. Komatsu *et. al.*, *Five-Year Wilkinson Microwave Anisotropy Probe (WMAP) Observations: Cosmological Interpretation*, Astrophys. J. Suppl. **180** (2009) 330–376, [[arXiv:0803.0547](#)].
- [6] **CDMS-II** Collaboration, Z. Ahmed *et. al.*, *Results from the Final Exposure of the CDMS II Experiment*, [[arXiv:0912.3592](#)].
- [7] R. Bernabei *et. al.*, *New results from DAMA/LIBRA*, [[arXiv:1002.1028](#)].
- [8] **CoGeNT** Collaboration, C. E. Aalseth *et. al.*, *Results from a Search for Light-Mass Dark Matter with a P-type Point Contact Germanium Detector*, [[arXiv:1002.4703](#)].

- [9] E. Aprile *et. al.*, *First Dark Matter Results from the XENON100 Experiment*, [arXiv:1005.0380](#).
- [10] C. McCabe, *The Astrophysical Uncertainties Of Dark Matter Direct Detection Experiments*, [arXiv:1005.0579](#).
- [11] J. I. Collar and D. N. McKinsey, *Comments on 'First Dark Matter Results from the XENON100 Experiment'*, [arXiv:1005.0838](#).
XENON Collaboration, *Reply to the Comments on the XENON100 First Dark Matter Results*, [arXiv:1005.2615](#).
J. I. Collar and D. N. McKinsey, *Response to arXiv:1005.2615*, [arXiv:1005.3723](#).
- [12] **Particle Data Group** Collaboration, C. Amsler *et. al.*, *Review of particle physics*, Phys. Lett. **B667** (2008) 1.
- [13] A. Boyarsky, J. Lesgourgues, O. Ruchayskiy, and M. Viel, *Lyman-alpha constraints on warm and on warm-plus-cold dark matter models*, JCAP **0905** (2009) 012, [[arXiv:0812.0010](#)].
- [14] P. D. Serpico and G. G. Raffelt, *MeV-mass dark matter and primordial nucleosynthesis*, Phys. Rev. **D70** (2004) 043526, [[astro-ph/0403417](#)].
- [15] G. 't Hooft, (ed.) *et. al.*, *Recent Developments in Gauge Theories. Proceedings, Nato Advanced Study Institute, Cargese, France, August 26 - September 8, 1979*, . New York, Usa: Plenum (1980) 438 P. (Nato Advanced Study Institutes Series: Series B, Physics, 59).
- [16] L. Lavoura, *General formulae for $f1 \rightarrow \gamma f2$ gamma*, Eur. Phys. J. **C29** (2003) 191–195, [[hep-ph/0302221](#)].
- [17] J. Adam *et. al.*, *A limit for the $\mu \rightarrow e \gamma$ decay from the MEG experiment*, Nucl. Phys. **B834** (2010) 1–12, [[arXiv:0908.2594](#)].
- [18] “Super-B factory.”
- [19] Y. Kuno and Y. Okada, *Muon decay and physics beyond the standard model*, Rev. Mod. Phys. **73** (2001) 151–202, [[hep-ph/9909265](#)].
- [20] S. Andreas, T. Hambye, and M. H. G. Tytgat, *WIMP dark matter, Higgs exchange and DAMA*, JCAP **0810** (2008) 034, [[arXiv:0808.0255](#)].
- [21] C. E. Yaguna, *Large contributions to dark matter annihilation from three-body final states*, [arXiv:1003.2730](#).
L. L. Honorez and C. E. Yaguna, *The inert doublet model of dark matter revisited*, [arXiv:1003.3125](#).
- [22] A. Djouadi, J. Kalinowski, and M. Spira, *HDECAY: A program for Higgs boson decays in the standard model and its supersymmetric extension*, Comput. Phys. Commun. **108** (1998) 56–74, [[hep-ph/9704448](#)].
- [23] G. Jungman, M. Kamionkowski, and K. Griest, *Supersymmetric dark matter*, Phys. Rept. **267** (1996) 195–373, [[hep-ph/9506380](#)].
- [24] D. Tucker-Smith and N. Weiner, *Inelastic dark matter*, Phys. Rev. **D64** (2001) 043502, [[hep-ph/0101138](#)].

- [25] R. Bernabei et. al., *Investigating the DAMA annual modulation data in the framework of inelastic dark matter*, Eur. Phys. J. **C23** (2002) 61–64.
D. Tucker-Smith and N. Weiner, *Inelastic dark matter at DAMA, CDMS and future experiments*, Nucl. Phys. Proc. Suppl. **124** (2003) 197–200, [[astro-ph/0208403](#)].
D. Tucker-Smith and N. Weiner, *The status of inelastic dark matter*, Phys. Rev. **D72** (2005) 063509, [[hep-ph/0402065](#)].
S. Chang, G. D. Kribs, D. Tucker-Smith, and N. Weiner, *Inelastic Dark Matter in Light of DAMA/LIBRA*, Phys. Rev. **D79** (2009) 043513, [[arXiv:0807.2250](#)].
J. March-Russell, C. McCabe, and M. McCullough, *Inelastic Dark Matter, Non-Standard Halos and the DAMA/LIBRA Results*, JHEP **05** (2009) 071, [[arXiv:0812.1931](#)].
D. S. M. Alves, S. R. Behbahani, P. Schuster, and J. G. Wacker, *Composite Inelastic Dark Matter*, [arXiv:0903.3945](#).
- [26] Y. Cui, D. E. Morrissey, D. Poland, and L. Randall, *Candidates for Inelastic Dark Matter*, JHEP **05** (2009) 076, [[arXiv:0901.0557](#)].
- [27] R. Bernabei et. al., *Investigating electron interacting dark matter*, Phys. Rev. **D77** (2008) 023506, [[arXiv:0712.0562](#)].
- [28] J. Kopp, V. Niro, T. Schwetz, and J. Zupan, *DAMA/LIBRA and leptonically interacting Dark Matter*, Phys. Rev. **D80** (2009) 083502, [[arXiv:0907.3159](#)].
- [29] **XENON10** Collaboration, J. Angle et. al., *Constraints on inelastic dark matter from XENON10*, Phys. Rev. **D80** (2009) 115005, [[arXiv:0910.3698](#)].
XENON Collaboration, J. Angle et. al., *First Results from the XENON10 Dark Matter Experiment at the Gran Sasso National Laboratory*, Phys. Rev. Lett. **100** (2008) 021303, [[arXiv:0706.0039](#)].
- [30] V. N. Lebedenko et. al., *Result from the First Science Run of the ZEPLIN-III Dark Matter Search Experiment*, Phys. Rev. **D80** (2009) 052010, [[arXiv:0812.1150](#)].
- [31] G. Angloher et. al., *Commissioning Run of the CRESST-II Dark Matter Search*, [arXiv:0809.1829](#).
- [32] **KIMS** Collaboration, H. S. Lee et. al., *Limits on WIMP-nucleon cross section with CsI(Tl) crystal detectors*, Phys. Rev. Lett. **99** (2007) 091301, [[arXiv:0704.0423](#)].
- [33] S. Archambault et. al., *Dark Matter Spin-Dependent Limits for WIMP Interactions on 19-F by PICASSO*, Phys. Lett. **B682** (2009) 185–192, [[arXiv:0907.0307](#)].
- [34] J. Kopp, T. Schwetz, and J. Zupan, *Global interpretation of direct Dark Matter searches after CDMS-II results*, JCAP **1002** (2010) 014, [[arXiv:0912.4264](#)].
- [35] A. L. Fitzpatrick, D. Hooper, and K. M. Zurek, *Implications of CoGeNT and DAMA for Light WIMP Dark Matter*, [arXiv:1003.0014](#).
- [36] S. Chang, J. Liu, A. Pierce, N. Weiner, and I. Yavin, *CoGeNT Interpretations*, [arXiv:1004.0697](#).
- [37] F. Petriello and K. M. Zurek, *DAMA and WIMP dark matter*, JHEP **09** (2008) 047, [[arXiv:0806.3989](#)].
- [38] K. Schmidt-Hoberg and M. W. Winkler, *Improved Constraints on Inelastic Dark Matter*, JCAP **0909** (2009) 010, [[arXiv:0907.3940](#)].

- [39] S. Nussinov, L.-T. Wang, and I. Yavin, *Capture of Inelastic Dark Matter in the Sun*, JCAP **0908** (2009) 037, [[arXiv:0905.1333](#)].
- [40] D. Hooper, J. I. Collar, J. Hall, and D. McKinsey, *A Consistent Dark Matter Interpretation For CoGeNT and DAMA/LIBRA*, [arXiv:1007.1005](#).
- [41] P. W. Graham, R. Harnik, S. Rajendran, and P. Saraswat, *Exothermic Dark Matter*, [arXiv:1004.0937](#).
- [42] “Xenon100 [<http://xenon.astro.columbia.edu/>].”
- [43] R. M. Crocker, N. F. Bell, C. Balazs, and D. I. Jones, *Radio and gamma-ray constraints on dark matter annihilation in the Galactic center*, Phys. Rev. **D81** (Feb., 2010) 063516, [[arXiv:1002.0229](#)].
Q. Yuan, P.-F. Yin, X.-J. Bi, X.-M. Zhang, and S.-H. Zhu, *Gamma rays and neutrinos from dark matter annihilation in galaxy clusters*, [arXiv:1002.0197](#).
M. Ackermann et. al., *Constraints on Dark Matter Annihilation in Clusters of Galaxies with the Fermi Large Area Telescope*, JCAP **1005** (2010) 025, [[arXiv:1002.2239](#)].
- [44] K. N. Abazajian, P. Agrawal, Z. Chacko, and C. Kilic, *Conservative Constraints on Dark Matter from the Fermi-LAT Isotropic Diffuse Gamma-Ray Background Spectrum*, [arXiv:1002.3820](#).
- [45] **Fermi-LAT** Collaboration, B. Lott, *New insight into gamma-ray blazars from the Fermi-LAT*, Int. J. Mod. Phys. **D19** (2010) 831–839.
- [46] Y. Cui, J. D. Mason, and L. Randall, *General Analysis of Antideuteron Searches for Dark Matter*, [arXiv:1006.0983](#).
- [47] O. Mena, S. Palomares-Ruiz, and S. Pascoli, *Reconstructing WIMP properties with neutrino detectors*, Phys. Lett. **B664** (2008) 92–96, [[arXiv:0706.3909](#)].
- [48] “Icecube [<http://icecube.wisc.edu/>].”
- [49] D. Hooper, F. Petriello, K. M. Zurek, and M. Kamionkowski, *The New DAMA Dark-Matter Window and Energetic-Neutrino Searches*, Phys. Rev. **D79** (2009) 015010, [[arXiv:0808.2464](#)].
- [50] M. Cirelli et. al., *Spectra of neutrinos from dark matter annihilations*, Nucl. Phys. **B727** (2005) 99–138, [[hep-ph/0506298](#)].
- [51] A. E. Erkoca, M. H. Reno, and I. Sarcevic, *Muon Fluxes From Dark Matter Annihilation*, Phys. Rev. **D80** (2009) 043514, [[arXiv:0906.4364](#)].
- [52] A. Menon, R. Morris, A. Pierce, and N. Weiner, *Capture and Indirect Detection of Inelastic Dark Matter*, [arXiv:0905.1847](#).
- [53] M. E. Peskin and T. Takeuchi, *Estimation of oblique electroweak corrections*, Phys. Rev. **D46** (1992) 381–409.
- [54] R. Barbieri, A. Pomarol, R. Rattazzi, and A. Strumia, *Electroweak symmetry breaking after LEP-1 and LEP-2*, Nucl. Phys. **B703** (2004) 127–146, [[hep-ph/0405040](#)].
- [55] G. Cacciapaglia, C. Csaki, G. Marandella, and A. Strumia, *The minimal set of electroweak precision parameters*, Phys. Rev. **D74** (2006) 033011, [[hep-ph/0604111](#)].

- [56] N. Maekawa, *Electroweak symmetry breaking by vector - like fermions' condensation with small S and T parameters*, Phys. Rev. **D52** (1995) 1684–1692.
- G. Cynolter and E. Lendvai, *Electroweak Precision Constraints on Vector-like Fermions*, Eur. Phys. J. **C58** (2008) 463–469, [[arXiv:0804.4080](#)].
- [57] M. J. Strassler and K. M. Zurek, *Discovering the Higgs through highly-displaced vertices*, Phys. Lett. **B661** (2008) 263–267, [[hep-ph/0605193](#)].
- [58] “Atlas detector [<http://atlas.ch/>].”
- [59] A. Esmaili and Y. Farzan, *On the Oscillation of Neutrinos Produced by the Annihilation of Dark Matter inside the Sun*, [arXiv:0912.4033](#).